

RF Project 761420/711626
Interim Technical Report

**the
ohio
state
university**

research foundation

**1314 kinnear road
columbus, ohio
43212**

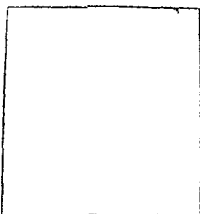
AN INVESTIGATION OF A MATHEMATICAL MODEL
FOR ATMOSPHERIC ABSORPTION SPECTRA

Edward R. Niple
Department of Physics

July, 1979

NATIONAL AERONAUTICS AND SPACE ADMINISTRATION
Washington, D. C. 20546

Grant No. NSG-7479



ACKNOWLEDGEMENTS

The author would like to express his thanks to Dr. John H. Shaw whose assistance and support was crucial to the completion of this report and the development of the ideas it contains.

TABLE OF CONTENTS

	<u>Page</u>
ACKNOWLEDGEMENTS	ii
LIST OF TABLES	iv
LIST OF FIGURES	v
ABSTRACT	vi
 <u>Chapter</u>	
I INTRODUCTION	1
II FUNDAMENTALS OF ATMOSPHERIC TRANSMITTANCE	3
A. Homogeneous Paths	3
B. Atmospheric Paths	4
C. Refraction Effects	5
D. Line Shape	8
E. Instrument Effects	9
1. Convolution Strategies	10
2. Romberg Integration	12
F. Verifying Calculation Behavior	15
III SOME INFORMATION ANALYSIS TECHNIQUES	27
A. Identifying "Bad" Parameters	27
B. Estimated Parameter Uncertainties	39
C. Low-Resolution Information Analysis	42
IV CONCLUSIONS	47
 APPENDICES	
A THE SPECTRUM CALCULATION PROGRAM	49
I. Main Program	49
II. Subroutine SNIDER	55
III. Subroutine PATHST	55
IV. Subroutine NSPEC	56
B THE LINE PARAMETER SETUP PROGRAM	75
REFERENCES	81

LIST OF TABLES

<u>Table</u>		<u>Page</u>
1	Comparison of path characteristics	16
2	Sample line parameters	18
3	Effect of different layer thicknesses	18
4	A sample T and M table for convolution routine	20
5	Convolution results for a sample Voigt line convolved with a Gaussian slit function	20
6	Convolution results for sample line with smaller frequency spacing	22
7	An example of a premature convergence	22
8	The T and M table for convolutions in Table 7	23
9	Parameter values used to compute sample spectra	29
10	Information matrices	35
11	Eigenvalues and associated eigenvectors of W^* from Table 10	36
12	Parameter steps producing a summed squared difference spectrum equal to 1, assuming Eq. (29) holds	37
13	Parameter uncertainties for various sets of parameter constraints, assuming an rms noise of 1%	41
14	Parameter values used to calculate low-resolution sample spectra	43
15	Parameter uncertainties for various sets of parameter constraints for low-resolution spectra, assuming an rms noise of 1%	45
16	Some eigenvectors and associated eigenvalues of modified information matrix for low-resolution spectra	46
A1	Inputs to main program	51
A2	Error codes for subroutine ERROR	53
A3	The number of points in the first trapezoidal evaluation for different values of NO	58

LIST OF FIGURES

<u>Figure</u>		Page
1	Observer-source geometry	6
2	Schematic representation of Eq. (17)	11
3	The Romberg T-table	13
4	Comparison with Kyle ²⁵ Spectrum	25
5	Comparison with Kyle ²⁵ Spectrum	26
6	Reference Spectrum	28
7	Spectrum for increased zenith angle — 95.4°, ---- 95.2° (reference spectrum)	30
8	(Reference spectrum) - (increased zenith angle spectrum)	31
9	Difference spectra for 2 K changes in the temperature in layers 41 and 42. — $\Delta T(41) = 2$ K, $\Delta T(42) = 0$, ---- $\Delta T(41) = 0$, $\Delta T(42) = 2$ K.	33
10	Low-resolution reference spectrum	44
A1	Overall program logic	50

ABSTRACT

A computer program that calculates absorption spectra for slant paths through the atmosphere is described. The program uses an efficient convolution technique (Romberg integration) to simulate instrument resolution effects. A brief information analysis is performed on a set of calculated spectra to illustrate how such techniques may be used to explore the quality of the information in a spectrum.

Blank
Page

I. INTRODUCTION

Radiation which has passed through and been modified by the atmosphere contains a wealth of information about atmospheric conditions. This includes information about the temperature and density structure of the atmosphere as well as the abundance and distribution of constituent gases and aerosols. In order to retrieve this information, however, an accurate model is needed which describes the dependence of absorption spectra on the atmospheric conditions and on the instrument characteristics. The first dependence has received considerable attention, both theoretical and computational, but the second has received much less. Equivalent width techniques and transmittance averaging are common ways of extracting information from spectra when instrument effects are unknown or poorly understood. However, because these effects mask underlying atmospheric effects, knowledge of the instrument behavior, when properly included in the data analysis, allows extraction of more detailed information than can be obtained in the absence of such knowledge.

Nonlinear least-squares¹ is one data analysis technique which can include all relevant influences on the data. It involves a great deal of computation, however, so efficient computer codes must be developed in order to take advantage of the least-squares techniques. This report describes a program for calculating absorption spectra that was specifically written to efficiently include instrument effects. It is therefore suitable for use in least-squares analysis.

In constructing a model for any experiment it is important to know what type of information the experimental data are likely to contain. Such knowledge allows the level of sophistication for the model to be balanced between computational complexity and interpretative accuracy. The third chapter of this report addresses this question and illustrates a variety of simple techniques for information analysis with a set of atmospheric absorption spectra.

Blank Page

2

II. FUNDAMENTALS OF ATMOSPHERIC TRANSMITTANCE

A beam of radiation propagating through the atmosphere is modified through the action of many different processes. Among these are scattering, reflection, refraction, polarization changes, atmospheric emission, and absorption. This report is only concerned with the modifications due to refraction and absorption by gas molecules in the atmosphere, and, in particular, that portion of the absorption due to rotational and vibrational transitions of the molecules. Each transition has associated with it a frequency position, width, intensity and profile. The Voigt profile^{2,3,23} is assumed throughout this report, although other shapes can be incorporated if desired.

A. HOMOGENEOUS PATHS

If radiation with a spectral irradiance $E(\nu)$ is incident on a homogeneous gas sample, the spectral radiant exitance $M(\nu)$ is given by⁴

$$M(\nu) = E(\nu) \cdot \tau(\nu) , \quad (1)$$

where ν is the frequency of the radiation measured in cm^{-1} . The modifying factor, $\tau(\nu)$, in Eq. (1) is called the spectral transmittance, which is referred to simply as transmittance in this report, it being understood that the transmittance is a function of frequency.

For a narrow homogeneous sample of thickness $d\ell$, Bouguer's law⁵ states that the radiation lost in the sample is linear in $E(\nu)$ and $d\ell$. Beer's law⁶ states that the radiation lost is also linear in the concentration N of the absorber, so that

$$dE(\nu, \ell) = -k(\nu) E(\nu, \ell) N d\ell , \quad (2)$$

where $k(\nu)$ is called the absorption coefficient. When N is measured in molecules/ cm^3 and $d\ell$ in cm, $k(\nu)$ is measured in $\text{cm}^2/\text{molecule}$. When N is independent of path length, Eq. (2) can be integrated over the entire path length, L , through the sample to give

$$M(\nu) = E(\nu, L) = E(\nu, 0) \exp[-k(\nu) NL] . \quad (3)$$

Consequently, the transmittance is given by

$$\tau(\nu) = \exp[-k(\nu) NL] . \quad (4)$$

Equation (2) is based on independent absorption by each absorbing molecule. It does not apply to self-broadening absorption, therefore, in which k can also depend on N . The factor in the exponential of Eq. (4) is called the absorbance.

If there are M different absorbers with concentrations N_1, N_2, \dots, N_M independently absorbing in the sample, the total absorbance $A(\nu)$ is

$$A(\nu) = \sum_{m=1}^M N_m k_m(\nu) L, \quad (5)$$

where $k_m(\nu)$ is the absorption coefficient for the m th absorber. As stated above, this report assumes that the absorption is due to many individual absorption lines, each with absorption coefficient $k_{mj}(\nu)$. Consequently Eq. (5) becomes

$$A(\nu) = L \cdot \sum_{m=1}^M N_m \cdot \sum_{j=1}^{J_m} k_{mj}(\nu), \quad (5b)$$

where J_m is the total number of lines for the m th absorber.

B. ATMOSPHERIC PATHS

Radiation paths in the atmosphere are usually not homogeneous. For such paths, Eq. (2) can still be integrated to give E as a function of path length, provided the variation of k and N with path length is known. The analog of Eq. (5) for atmospheric paths is

$$A(\nu) = \int_0^L \sum_{m=1}^M N_m(\ell) \sum_{j=1}^{J_m} k_{mj}(\nu, \ell) d\ell. \quad (6)$$

It is convenient to define the mixing ratio $a_m(\ell)$ for the m th absorber as

$$a_m(\ell) = N_m(\ell) / \bar{N}(\ell),$$

where $\bar{N}(\ell)$ is the mean density of the atmosphere as a function of path length.

Defining a new variable $u(\ell)$, the so-called airmass along the path, by

$$du \equiv \bar{N}(\ell) d\ell,$$

Eq. (6) becomes

$$A(\nu) = \int_0^U \sum_{m=1}^M a_m(u) \sum_{j=1}^{J_m} k_{mj}(\nu, u) du, \quad (7)$$

where

$$U \equiv \int_0^L \bar{N}(\ell) d\ell$$

is the total airmass of the path.

C. REFRACTION EFFECTS

This report uses a program written by Treve^{7,8} and Snider⁹ to determine the path of radiation through the atmosphere. The necessary geometry is shown in Fig. 1, assuming that the sun is the radiation source. The observer is at a height H_{ob} above the surface of the earth at latitude ϕ . The direction of propagation of the radiation makes an angle θ' with the observer's local zenith. A straight line drawn from the observer to the source makes an angle θ with the local zenith and has a minimum height H'_{min} above the surface of the earth. Because of refraction, the true radiation path is not straight and has a different minimum height H_{min} . The actual path taken by the radiation depends on the density profile of the atmosphere as a function of height. This profile is calculated by the program from an input temperature profile and base level pressure by integrating the hydrostatic equation and assuming an ideal gas law for the relationship between pressure, temperature, and density.¹⁰ The input profile is in the form of many thin atmospheric layers. The program uses Snell's law and the Lorentz-Lorenz relation to perform a ray-tracing through the layers. The output consists of a series of airmass values, effective temperatures, and pressures, one for each layer crossed by the ray.

In order to use these to calculate the spectrum, the integral in Eq. (7) is approximated by a sum according to

$$A(\nu) = \int_0^U \sum_{m=1}^M a_m(u) \sum_{j=1}^{J_m} k_{mj}(\nu, u) du$$

$$\approx \sum_{i=1}^{I_L} \sum_{m=1}^M \sum_{j=1}^{J_m} \left[\overline{a_m k_{mj}(\nu)} \right]_i \Delta u_i, \quad (8)$$

where I_L is the number of terms in the sum which replaces the integral in Eq. (7).

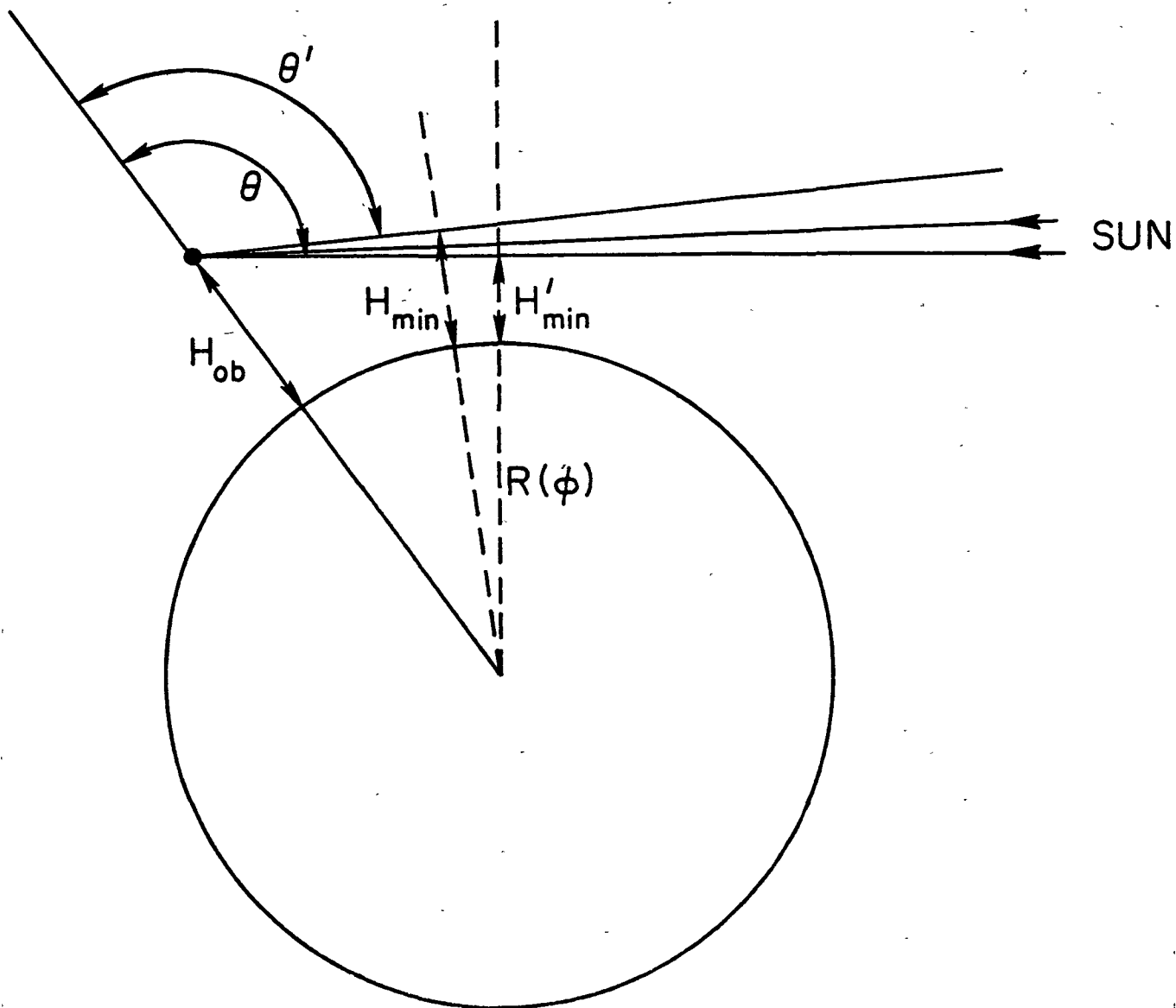
The form of $\left[\overline{a_m k_{mj}(\nu)} \right]_i$ is determined by assuming that the product $a_m(u) k_{mj}(\nu, u)$ for fixed ν can be written as a function of the pressure $P(u)$ and temperature $T(u)$ along the path. We therefore write

$$\int a_m(u) k_{mj}(\nu, u) du = \int f[P(u), T(u)] du.$$

Expanding f in a Taylor series about some value, P_0, T_0 ,

$$f(P, T) = f(P_0, T_0) + \left. \frac{\partial f}{\partial P} \right|_{P_0, T_0} (P - P_0) + \left. \frac{\partial f}{\partial T} \right|_{P_0, T_0} (T - T_0) + \{\text{second-order terms}\}.$$

Substituting this expression into the integral



θ = "true" or astronomical zenith angle
 θ' = apparent zenith angle
 H_{ob} = observer height
 H'_{min} = unrefracted minimum height
 H_{min} = true minimum height
 $R(\phi)$ = radius of earth at latitude ϕ

Fig. 1 - Observer-source geometry

$$\begin{aligned}
\int f[P(u), T(u)] du &= f(P_0, T_0) \int du \\
&+ \left. \frac{\partial f}{\partial P} \right|_{P_0, T_0} \int (P - P_0) du + \left. \frac{\partial f}{\partial T} \right|_{P_0, T_0} \int [T(u) - T_0] du \\
&+ \{\text{second-order terms}\} \\
&= \left[f(P_0, T_0) + \left. \frac{\partial f}{\partial P} \right|_{P_0, T_0} (\bar{P} - P_0) + \left. \frac{\partial f}{\partial T} \right|_{P_0, T_0} (\bar{T} - T_0) \right. \\
&\quad \left. + \{\text{second-order terms}\} \right] \int du,
\end{aligned}$$

where

$$\bar{P} \equiv \int P(u) du / \int du$$

and

$$\bar{T} \equiv \int T(u) du / \int du.$$

(9)

But the expression in the brackets, to first-order, is just $f(\bar{P}, \bar{T})$. Consequently, provided the variation of $P(u)$ and $T(u)$ is sufficiently small that the first-order terms in the Taylor series are adequate, we may write

$$\int f[P(u), T(u)] du \approx f(\bar{P}, \bar{T}) \Delta u, \quad (10)$$

where \bar{T} and \bar{P} are defined as in Eq. (9).

If the atmospheric layers are sufficiently thin, we are therefore justified in replacing the integral in Eq. (7) with the sum in Eq. (8) provided

$$\left[\overline{a_m k_{mj}(\nu)} \right]_i = a_m(\bar{P}_i, \bar{T}_i) k_{mj}(\bar{P}_i, \bar{T}_i, \nu), \quad (11)$$

where

$$\bar{P}_i \equiv \int_{\text{layer } i} P(u) du / \Delta u_i$$

and

(12)

$$\bar{T}_i \equiv \int_{\text{layer } i} T(u) du / \Delta u_i.$$

Equations (11) and (12) are close to the familiar scaling approximations.¹¹ The same argument applies to any other variables that effect the $a \cdot k$ product (such as mixing ratio dependence in k). One can therefore approximate the inhomogeneous atmosphere with a series of homogeneous layers whose properties are given by averages over the true inhomogeneous variation.

D. LINE SHAPE

As stated above, this report assumes that the absorption coefficient $k_{mj}(\nu)$ follows the Voigt profile. This profile combines the effects of collision broadening (which is dominant in the troposphere) and Doppler broadening (which is dominant in the upper stratosphere). It is given by

$$k_{mj}(\nu, P, T) = k_{0jm} \frac{y}{\pi} \int_{-\infty}^{\infty} \frac{\exp(-t^2) dt}{y^2 + (x - t)^2}, \quad (13)$$

where

$$k_{0jm} = \frac{S_{jm}}{\alpha_D} \sqrt{\ln 2 / \pi},$$

$$y = \frac{\alpha_L}{\alpha_D} \sqrt{\ln 2}, \text{ and}$$

$$x = \frac{\nu - \nu_{0jm}}{\alpha_D} \sqrt{\ln 2}.$$

The line intensity S_{jm} is defined as $S_{jm} = \int_0^{\infty} k_{jm}(\nu) d\nu$.

From Quantum Mechanics¹² this quantity is given by

$$S_{jm} = \frac{8\pi^3 \nu_{0jm}}{3hc} \frac{g''(1 - e^{-hc\nu_{0jm}/kT})}{Q_m(T)} \exp[(-E''_{mj})/kT] \cdot |\langle \psi''_{jm} | \vec{\mu} | \psi'_{jm} \rangle|^2. \quad (14)$$

In this expression, ν_{0jm} is the line center frequency for the m th line with lower state energy E''_{mj} and upperstate energy $E'_{mj} = hc\nu_{0jm} + E''_{mj}$. g'' is the degeneracy of the lower state and $Q_m(T)$ is the partition function. In the infrared, the expression $\frac{1 - \exp(-hc\nu_{0jm}/kT)}{Q_m(T)}$ can usually be approximated by $1/Q_{rot}(T)$ where $Q_{rot}(T)$, the rotational partition function, is proportional¹³ to T for linear molecules such as CO, N₂O, CO₂, and NO. It is proportional to $T^{3/2}$ for molecules like O₃, H₂O, and CH₄. The term $|\langle \psi''_{jm} | \vec{\mu} | \psi'_{jm} \rangle|^2$ is the square of the dipole matrix element.

The temperature dependence of S_{jm} is made explicit by writing it as

$$S_{jm} = S_{0jm} \left(\frac{T_0}{T} \right)^\beta \exp[-E''_{mj}(T_0 - T)/0.6946TT_0] , \quad (15)$$

where $\beta = 1$ or $3/2$ depending on the molecular structure. The above expression assumes that E is measured in cm^{-1} and T in Kelvin. S_{0jm} is the value of S_{jm} at some standard temperature, T_0 .

The quantities α_L and α_D in Eq. (13) are the Lorentz width and Doppler width of the line, respectively. These are given by

$$\alpha_D = \frac{v_{0mj}}{c} \sqrt{\frac{2kT \ln 2}{M_m}} \quad \text{and} \quad (16)$$

$$\alpha_L = \alpha_{0mj} \left(\frac{T_0}{T} \right)^\gamma \frac{P_0}{P} .$$

M_m is the mass of molecular species m ; α_{0mj} is the Lorentz width at some standard temperature and pressure, T_0 and P_0 ; and γ is an empirical term describing the temperature dependence of α_L . This report makes the standard assumption that $\gamma = 1/2$ although other values are often more accurate for bands of specific molecules. The necessary line parameters were taken from the AFGL line listing.¹⁴

E. INSTRUMENT EFFECTS

When Eq. (13) and (8) are combined, they constitute a mathematical model for the frequency make-up of a beam of radiation as it propagates through the atmosphere. Since real spectrometers have finite resolution, the signal observed at frequency setting ν is a weighted sum of the radiation incident on the instrument. This is described by writing

$$\tau_{\text{con}}(\nu) = \int_0^\infty \sigma(\nu, \nu') \tau_{\text{mon}}(\nu') d\nu' , \quad (17)$$

where $\tau_{\text{con}}(\nu)$ is the observed transmittance, $\tau_{\text{mon}}(\nu')$ is the monochromatic transmittance, and $\sigma(\nu, \nu')$ is the instrument spectral response function (or "slit" function) with

$$\int_0^\infty \sigma(\nu, \nu') d\nu' = 1 .$$

It is often assumed that σ can be written as a function of $(\nu - \nu')$, and many different forms are used. For grating instruments, triangular and Gaussian shapes are common,¹⁵ and for interferometers sinc, sinc², and various Bessel functions have been tried,¹⁶ depending upon the apodization.

When calculated and observed spectra are to be compared visually, the exact form of σ is often unimportant. However, when more sensitive

techniques, such as least-squares analysis, are used, instrument effects must be modeled with a precision at least better than the precision of the observed spectral values. This imposes an additional set of computational restrictions on spectrum calculation routines, especially when the convolution integral in Eq. (17) must be evaluated numerically, as is usually the case. While considerable effort has gone into devising efficient algorithms for calculating monochromatic transmittances, little work seems to have been done on the special problems associated with calculating convolved transmittances.

Since one of the problems this report seeks to address is the applicability of least-squares data analysis to atmospheric transmission spectra, the precision of convolved transmittances has been a central concern from the start. To see how this concern dictates the overall calculation strategy, consider how Eq. (17) is evaluated in practice. Because of the complex frequency dependence of $\tau(\nu')$, the integral must be evaluated numerically; i.e., replaced by a weighted sum. Each term in the sum requires a value of τ_{mon} and one of σ . If N_c is the number of terms in the sum and N_s is the number of observed spectral values, then $N_c \cdot N_s$ monochromatic transmittance values are needed to calculate the convolved transmittance, τ_{con} .

A typical frequency position may have contributions from 20 different lines and require 20 atmospheric layers to model the atmosphere (Mankin¹⁷ used ~1000 lines over a 10 cm^{-1} region; Snider and Goldman¹⁰ used 197 layers). In addition, if the resolution is $\delta\nu_R$ a typical frequency spacing for observed spectra is $\delta\nu_R/2$. Consequently for a 200 cm^{-1} -long spectrum at moderate resolution, $\delta\nu_R = 0.10 \text{ cm}^{-1}$ (some interferometers have 10 times better resolution), a total of 4000 observed points must be calculated. Assuming that the most time-consuming part of the calculation is the evaluation of the Voigt profile, a total of $N_c \times 20 \times 20 \times 4000 = 1.6 \times 10^6 N_c$ Voigt evaluations must be performed. Running time is dependent on machine characteristics, but Pierluissi and Vanderwood¹⁸ quote a time of ~3 seconds for 100 evaluations on an IBM 360/65. This gives $4.8 \times 10^4 \cdot N_c$ seconds of CPU time in the Voigt routine alone. Clearly N_c must be made as small as possible.

1. Convolution Strategies

The numerical evaluation of the integral in Eq. (17) is represented schematically in Fig. 2. To each observed frequency position ν_i there corresponds a set of frequency positions $\{\nu'\}_i$ at which monochromatic transmittances must be calculated. Clearly the number of points ν' can be reduced by making some of the $\{\nu'\}_{i+1}$ points overlap some of the $\{\nu'\}_i$ points. However, because the number of $\{\nu'\}_i$ values needed for a given level of accuracy ϵ in $\tau_{\text{con}}(\nu_i)$ depends upon the form of the monochromatic transmittance, the density of $\{\nu'\}_i$ points will be a function of ν_i for a given ϵ . The exact density depends on the numerical integration rule employed, but usually this takes the form of bounds on the magnitude of high-order derivatives of τ_{mon} over the convolution frequency range. The use of an iterative quadrature routine can often eliminate the need for

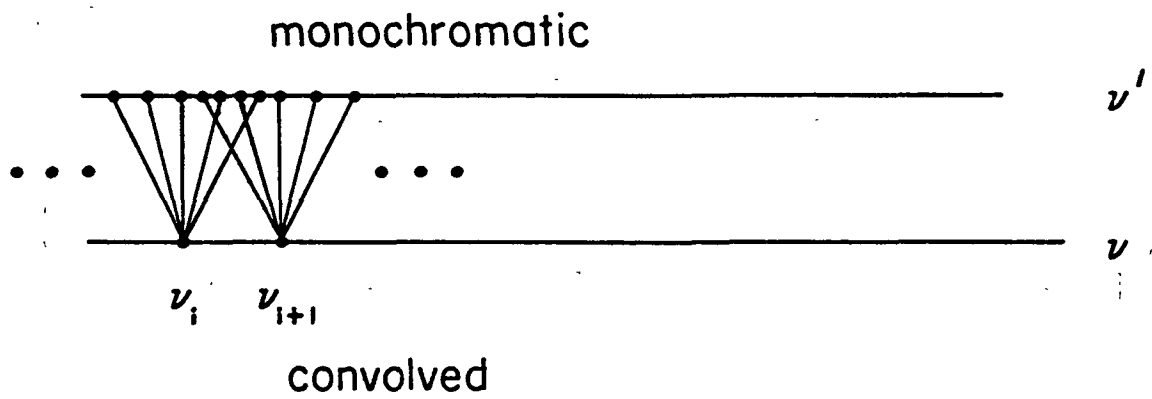


Fig. 2 - Schematic representation of Eq. (17)

evaluating these derivatives. Also, if the $\tau_{\text{con}}(\nu_i)$ values are calculated in order of increasing [or decreasing] frequency position, values of τ_{mon} at frequencies lower [higher] than the i th range of ν' values need not be saved. This reduces storage requirements.

Of the many available iterative routines, an equally spaced abscissa Romberg integration algorithm was selected. Gaussian rules require fewer $\{\nu'\}$ points for a given ϵ , but are not well adapted to iterative evaluation. Neither are they well suited for overlapping $\{\nu'\}$ positions for successive ν_i values. Adaptive Simpson's rule techniques are good at varying the ν' -density to meet the accuracy requirements and could be written so as to use overlapping $\{\nu'\}$ positions. Unfortunately they are much more complicated than Romberg schemes, which proved to be complicated enough. Better programmers than the author of this report may wish to use them, however.

2. Romberg Integration

To use classical Romberg integration to evaluate the integral

$$I \equiv \int_a^b f(X) dx$$

the interval $[a, b]$ is divided into 2^{k_0} equal pieces. The function f is evaluated at each of the $2^{k_0} + 1$ points,

$$x_i = a + (i - 1)(b - a)/2^{k_0} \quad i = 1, \dots, 2^{k_0} + 1,$$

and the sum,

$$\begin{aligned} T_0^{(k_0)} = \frac{(b - a)}{2^{k_0}} & \left[\frac{1}{2} f(x_1 = a) + f(x_2) + \dots \right. \\ & \left. + f(x_{2^{k_0}}) + \frac{1}{2} f(x_{2^{k_0}+1} = b) \right], \end{aligned} \quad (18)$$

forms the first element of a table of approximations to I called the Romberg T-table. Equation (18) is easily recognized as the trapezoidal rule. Next, k_0 is replaced by $k_1 = k_0 + 1$ and $T_0^{(k_1)}$ is calculated from Eq. (18) with k_0 replaced by k_1 . This value forms a second estimate for I and is written next to $T_0^{(k_0)}$ in the top-most row of the table, as shown in Fig. 3. From these two estimates a third estimate, $T_1^{(k_0)}$, is formed according to

$$T_m^{(k)} = \frac{4^{m-1} T_{m-1}^{(k+1)} - T_{m-1}^{(k)}}{4^m - 1}. \quad (19)$$

$T_0^{(k_0)}$	$T_0^{(k_1)}$	$T_0^{(k_2)}$. . .
	$T_1^{(k_0)}$	$T_1^{(k_1)}$. . .
		$T_2^{(k_0)}$. . .
			.
			.
			.

Fig. 3 - The Romberg T-table

The values of $T_0^{(k_0)}$ and $T_1^{(k_0)}$ are then compared, and if

$$\left| T_1^{(k_0)} - T_0^{(k_0)} \right| < \epsilon, \quad (20)$$

the process stops and outputs $T_1^{(k_0)}$ as the final approximation to I . If the convergence criterion in Eq. (20) is not satisfied, the table construction continues with $T_0^{(k_2)}$, $T_0^{(k_3)}$ and so on until two successive elements along the diagonal of the table do satisfy the convergence criterion.

Davis and Rabinowitz¹⁹ discuss a modification of the classical Romberg scheme which requires calculation of a second table, the Romberg M-table. In this scheme, after $T_0^{(k_0)}$ is calculated, the quantity

$$M_0^{(k_0)} = \frac{b-a}{2^{k_0}} \sum_{j=1}^{2^{k_0}} f \left[a + \left(j - \frac{1}{2} \right) (b-a)/2^{k_0} \right] \quad (21)$$

is calculated. Equation (21) is easily recognized as the midpoint rule. The values of $T_0^{(k_0)}$ and $M_0^{(k_0)}$ are then compared and if

$$\left| M_0^{(k_0)} - T_0^{(k_0)} \right| < \epsilon, \quad (22)$$

the process stops and outputs

$$T_0^{(k_1)} = \frac{1}{2} \left(T_0^{(k_0)} + M_0^{(k_0)} \right) \quad (23)$$

as the final approximation to I . If the new convergence criterion [Eq. (22)] is not met, the next diagonal element of the T-table is calculated from

$$T_m^{(k)} = M_{m-1}^{(k)} + \frac{(2 \cdot 4^{m-1} - 1)(T_{m-1}^{(k)} - M_{m-1}^{(k)})}{4^m - 1}. \quad (24)$$

The next element of the M-table, $M_0^{(k_1)}$, is calculated from Eq. (21) with k_0 replaced by $k_1 = k_0 + 1$. The two M values are then combined as in Eq. (19) to form $M_1^{(k_0)}$. The convergence criterion is then applied to $M_1^{(k_0)}$ and $T_1^{(k_0)}$. If the criterion is satisfied, these two are combined as in Eq. (23) and output. Otherwise the process continues halving the interval $[a,b]$ and recursively generating the T- and M-tables until two corresponding diagonal elements satisfy the convergence criterion.

Those referring to Davis and Rabinowitz¹⁹ should note that Eq. (6.3.9) in their book is incorrect in some editions, as can be verified from their

Eq. (6.3.8) and the equation below (6.3.2). Also, the FORTRAN version of this technique, incorporated into the program in Appendix A, has a maximum number of interval halvings in the search for convergence. When this limit is exceeded, the output is taken from Eq. (24) rather than Eq. (23).

Incorporating the Romberg Table evaluation in the spectrum calculation routine required less than 15 FORTRAN statements. The logic needed to save τ_{mon} values required nearly 10 times as many statements. The details are given in Appendix A.

F. VERIFYING CALCULATION BEHAVIOR

The program which evaluates Eq. (17), described in Appendix A, is composed of three basic parts: (1) evaluation of the atmospheric path (subroutine SNIDER), (2) setting up approximate layer parameters (subroutine PATHST), and (3) spectrum calculation (subroutine NSPEC). These were first checked individually and then as a whole.

A specific observer-source geometry was selected. This had an observer at 45° N latitude, 45 km height, and an observed zenith angle (θ' in Fig. 1) of 95.2° . The source was assumed to be above the atmosphere. Unfortunately, the atmospheric model used by Snider and Goldman¹⁰ could not be obtained so the January reference atmosphere of Cole and Kantor²⁰ was used instead. The program's analysis of the path is shown in Table 1' along with the associated results taken from Ref. (10). Also shown are the results using a 190-layer atmosphere taken from the U.S. Standard Atmosphere, 1976.²¹ The agreement shown in the table and the proper behavior of the subroutine to changes in zenith angle, observer height, and ground-level pressure indicated that the subroutine was functioning properly.

The output for the 190-layer model included 198 sets of (u_i , \bar{T}_i , \bar{P}_i) values; 59 values for layers crossed in the portion of the path going from the observer in layer #99 to the minimum height in layer #41, and 139 values for layers crossed in the portion from the minimum height to the top of the atmosphere. The average layer thickness in this model is ~ 4 km. Examination of these 198 sets showed that of the 1.200099×10^{26} mol/cm² in the path, 3.1341×10^{25} , or 26%, were in the 0.35 km thick portion of layer 41 that contains the lowest segment of the path. This demonstrates the height selective nature of the limb geometry.

Compare this to the result obtained by Schmidt²² that a uniform error of 0.5 km in the minimum height of a limb emission spectrum produced a 21% rms error in retrieved mixing ratios (using simulated balloon data).

The next highest layer, #42, contained 1.4154×10^{25} mol/cm², or 11.8%. A full 60% of the air mass lay between 18.45 and 20.49 km.

Next the Voigt function evaluation routine, due to Hui, Armstrong, and Wray,²³ was checked against the tables of Young.²⁴ It gave good agreement over the tabulated range of x and y values. A set of sample

Table 1. Comparison of path characteristics.

	Ref. (20)	Ref. (10)	Ref. (21)
Apparent Zenith angle (degrees)	95.2	95.2	95.2
Lower height (m)	45000.0	45000.0	45000.0
Upper height (m)	89999.9	99000.0	82000.0
Minimum height (m)	18454.5	18434.1	18450.0
Chapman airmass	6.168	7.098	6.385
Optical airmass	5.422	6.085	5.573
HDIFF (m)	1000.5	1138.5	1030.0
Refraction (degrees)	0.11255	0.12788	0.11579
Astronomical Zenith angle (degrees)	95.31	95.33	95.32
P(EFF) (N/m^2)	4518.41	5494.93	4999.92
T(EFF) (K)	216.26	219.54	218.93
P(TAN) (N/m^2)	7890.17	9066.33	

line parameters were then chosen. These are shown in Table 2. A uniform mixing ratio of 0.1 ppm was used to calculate the absorbance in each layer.

The total absorbance was 1.231378 at $\nu = \nu_0 = 2090.796 \text{ cm}^{-1}$, corresponding to a transmittance (no convolution) of 0.29189. The absorbance in layer 41 was 0.197407, or ~16%, and the absorbance between 18.45 and 20.49 km was 0.456708, or 37%. These values show that the absorbance at line center is less peaked with height than the airmass. For Lorentz-like lines, the absorbance at ν_0 is Su/α . Consequently the decrease in u with height is offset by the decrease in α (because of decreasing pressure) and the absorbance is "smeared out" with height. The degree of Lorentz-like behavior for Voigt lines is determined by y in Eq. (13). Large y implies a high degree of Lorentz-like behavior; small y implies mainly Doppler-like behavior. The Lorentz-Doppler crossover point, $y \approx 1$, occurs at layer 63 for the sample line and atmospheric profile used; consequently, the observed "smearing" is reasonable.

The above observations suggest that high-resolution spectra should have better height sensitivity than low-resolution spectra because the same effect which "smears" the line center absorbance sharpens the wing absorbance, which goes as $Su\alpha$. In low-resolution spectra the observed signal is a mix of the two and has intermediate height sensitivity. High-resolution spectra are better to use to study the height-sensitive wing absorbance.

A second consequence of the "smearing" is found when the fine layers are combined into thicker layers. Let consecutive layers $\ell_1, \ell_2, \dots, \ell_n$ with parameters $(u_1, \bar{T}_1, \bar{P}_1), \dots, (u_n, \bar{T}_n, \bar{P}_n)$ be combined into one layer with parameters

$$\begin{aligned} u &\equiv \sum_{i=1}^n u_i , \\ \bar{T} &\equiv \sum u_i \bar{T}_i / u , \text{ and} \\ \bar{P} &\equiv \sum u_i \bar{P}_i / u . \end{aligned} \tag{25}$$

The new layer represents a less accurate approximation to the atmosphere than the original layers. In order to save computation time, it is desirable to use the minimum number of layers to calculate the spectrum. Subroutine SNIDER is sufficiently fast, however, that no such concerns apply to it. To test the sensitivity of the calculated spectrum to the layer coarseness, the original 139 sets of (u, \bar{T}, \bar{P}) , one for each layer crossed, were combined into segments of approximately equal airmass. Each new layer had an airmass as close to, but less than, U/N_{ge} as possible, where N_{ge} is some integer. The calculated absorbances at three different frequencies for several different values of N_{ge} are shown in Table 3. It is clear from these results that more layers are required at line center than in the wings. This is because the result of decreasing N_{ge} is to

Table 2. Sample line parameters*

$\nu_0 = 2090.796 \text{ cm}^{-1}$
$S_0 = 0.189 \times 10^{-20} \text{ mol}^{-1} \text{ cm}$
$\alpha_0 = 0.110 \text{ cm}^{-1}$
$E'' = 272.220 \text{ cm}^{-1}$
$m = 48 \text{ amu}$

*corresponding to the (6,13)-(6,14) line of the $\nu_1 + \nu_3$ band of $^{16}\text{O}_3$.

Table 3. Effect of different layer thicknesses.

$\nu(\text{cm}^{-1})$	Nge	# Layers	A(ν)
2090.796	3	3	1.12296698
2090.796	9	7	1.20571646
2090.796	35	18	1.22967891
2090.796	-	139	1.231378
2090.806	3	3	0.204556963
2090.806	9	7	0.202129669
2090.806	35	18	0.20184368
2090.806	-	139	0.201829374
2090.816	3	3	0.0613707937
2090.816	9	7	0.0616293664
2090.816	35	18	0.0614016373
2090.816	-	139	0.0613723083

produce thicker layers in the upper portions of the atmosphere where the u_i values are small. Since the line center absorbance is more sensitive to these upper layers, the loss of detail has more effect on it than wing absorbance values.

The program in Appendix A includes a subroutine called PATHST which performs the layer combination. The parameter Nge is used to set the fineness of the layers used to calculate the spectrum. As written, however, the subroutine combines the layers in such a way that each has an airmass at least as great as U/Nge but as close to U/Nge as possible. For the spectra in the next section, a value of $Nge = 15$ was found to be acceptable, but Table 3 indicates that different values may be required for different types of spectra.

The convolution portion of the program was tested on a flat ($\partial\tau/\partial\nu = 0$) spectral region with a Gaussian slit function of the form

$$\sigma_{\text{Gauss}}(\nu - \nu') = \frac{\sqrt{\ln 2}}{H\sqrt{\pi}} \exp\left[-\frac{(\nu' - \nu)^2 \ln 2}{H^2}\right]. \quad (26)$$

A five-point initial trapezoidal evaluation was used to start the Romberg iterations with a frequency extent of $8H$. The T and M table entries calculated for one run are shown in Table 4. A convergence criterion corresponding to 1% between the respective T and M table elements [see Eq. (22)] was used. Only the diagonal of the T-table is shown since the other elements are not calculated in the modified routine. The table elements must be multiplied by 2 to get the corresponding transmittance values. In this example, the routine went two iterations beyond the initial trapezoidal and midpoint evaluations before converging. The final value shows excellent agreement with the true value.

The routine was also tried on a Voigt line with parameters

$$\nu_0 = 2875.90 \text{ cm}^{-1}$$

$$S_0 = 0.0668 \text{ atm}^{-1} \text{ cm}^{-1}/\text{cm}$$

$$\alpha_{L_0} = 0.023176 \text{ cm}^{-1}$$

$$E'' = 400.00 \text{ cm}^{-1}$$

$$m = 36 \text{ amu}$$

at a uniform pressure of 1 atm and temperature of 300 K. The total airmass was $u = 200 \text{ atm cm}$. Table 5 shows the results for 10 different observed frequency positions spaced 0.2 cm^{-1} apart. The second column gives the calculated transmittance values with $\epsilon = 0.01$, $H = 0.083819 \text{ cm}^{-1}$, and an initial five-point trapezoidal evaluation that extended $2\frac{1}{2} H$ on either side of the central position. By comparing values equally spaced around 2875.90 cm^{-1} the consistency is seen to be ~ 0.001 , which is $\epsilon/10$. The

Table 4. A sample T and M table for convolution routine. (Table values must be multiplied by 2 to give transmittance value.)

TRAP	MID	Iteration	
		1	2
0.5284401	0.471553	0.4999984	0.4999976
0.4905153		0.5094798	0.4999971
0.5006297			0.4993649

$$\tau = 0.9999946 \quad (\text{exact} = 1.0000000)$$

Table 5. Convolution results for a sample Voigt line convolved with a Gaussian slit function.

$\nu \text{ (cm}^{-1}\text{)}$	τ_{con}	Iterations	Total Points	New Points
2875.00	0.9984500	1	9	9
2875.20	0.9952382	1	9	3
2875.40	0.9944796	1	9	4
2875.60	0.9885907	1	9	4
2875.80	0.8511999	3	33	29
2876.00	0.8508019	2	17	8
2876.20	0.9872358	1	9	3
2876.40	0.9942334	1	9	4
2876.60	0.9960335	1	9	4
2876.80	0.9964244	1	9	4
				TOTAL 72

third column lists the number of iterations required for convergence of the convolution integral. A value of 1 means that the convergence criterion was satisfied on the first try. The fourth column lists the number of monochromatic transmittances required for the convolution, and the fifth column lists the number of new monochromatic transmittance values calculated at each observed frequency. The increased density of points around line center, where the monochromatic transmittance changes most rapidly, is apparent.

Table 6 shows similar results for the identical spectrum except with a smaller frequency spacing. The fifth column shows the larger savings in calculations for more closely spaced observed frequencies. For reference, the 10 points in Table 6 took 0.09 second of cpu time to execute. This corresponds to 1.7 ms per monochromatic transmittance calculation. A later sample spectrum including 55 atmospheric layers and 13 lines, averaged 0.15 ms per monochromatic transmittance calculation on the OSU Amdahl Computer.

Sample spectra for other sets of line parameters produced similar results. It was found that extremely narrow and strong lines required considerably more iterations than broad lines. This can lead to unreasonably high numbers of iterations unless some maximum number of iterations is specified; usually a value of 7 was used. When convergence does not occur on the seventh iteration, the program outputs the most recent element of the T-table, sets an error flag, and proceeds to the next frequency position.

A variety of other tests were performed on the program, including the effect of different convergence criterion values. More is said about this in the next chapter. Overall the behavior was found to be satisfactory but one persistent problem did arise; it was found that the convolution routine would often converge prematurely. An example is shown in Table 7. The rapid decrease in the number of iterations, in a spectral region where the transmittance is not changing much, indicates a premature convergence. This is verified in the T- and M-tables for these two points shown in Table 8. The boxed portions correspond to the values in Table 7 where the convergence criterion was 0.005 (or 0.5%). The larger values in Table 8 correspond to a convergence criterion of 0.0001 (or 0.01%). The premature convergence at 1900.05 cm^{-1} is seen to be due to a misleading resemblance between the first T- and M-values. Subsequent iterations show the true value to be considerably lower than these, which the more stringent convergence criterion has picked up. This type of behavior is often encountered in iterative procedures. This problem was only detected when the slit function width was much larger than the line widths, though in principle it could occur in other situations. It was found that the problem could usually be avoided by adjusting the convergence criterion and the number of points in the first trapezoidal evaluation. The parameters can only be set based on experience and knowledge of the spectral region, and those lacking both these should indicate some caution.

Table 6. Convolution results for sample line with smaller frequency spacing.

$\nu(\text{cm}^{-1})$	τ_{con}	Iterations	Total Points	New Points
2875.70	0.9694133	1	9	9
2875.74	0.9396371	1	9	0
2875.78	0.8870856	2	17	10
2875.82	0.8118306	3	33	18
2875.86	0.7381039	3	33	3
2875.90	0.7074896	3	33	3
2875.94	0.7380002	3	33	3
2875.98	0.8117288	3	33	3
2876.02	0.8863926	3	33	3
2876.06	0.9391911	2	17	1
				<hr/> TOTAL 53

Table 7. An example of a premature convergence.

$\nu(\text{cm}^{-1})$	τ_{con}	Iterations
1900.00	0.96867	5
1900.05	0.99230	1

Table 8. The T- and M-tables for convolutions in Table 7. (Boxed portions correspond to a convergence criterion of 0.005. Entire tables for convergence criterion of 0.0001. Multiply table values by 0.0625 to get transmittance.)

TRAP	MID	$\nu = 1900.00 \text{ cm}^{-1}$			
15.85111	15.72414	14.90784	15.61850	15.52610	15.49732
15.77746		14.63574	15.85539	15.49529	15.48772
15.16341			15.93670	15.47128	15.48721
15.55619				15.46389	15.48746
15.50986					15.48755
15.49869					15.49775

TRAP	MID	$\nu = 1900.05 \text{ cm}^{-1}$			
15.87981	15.87390	15.74799	15.85101	15.83745	15.83456
15.87587		15.70601	15.88535	15.83293	15.83359
15.78528			15.89730	15.82943	15.83364
15.84218				15.82835	15.83370
15.83524					15.83372

As a final check on the entire calculation routine, two sample spectra were calculated under conditions similar to those used by Kyle and Goldman.²⁵ The observer was at a height of 4 km with the sun overhead. The spectra for the 1900-1902 cm^{-1} and 1930-1935 cm^{-1} regions are shown in Figs. 4 and 5, respectively. There are some differences in the conditions between these spectra and the corresponding high-resolution spectra of Kyle. Both have an instrument resolution of 0.1 cm^{-1} but Kyle used a triangular slit function and we used a Gaussian. Also, the values of the CO_2 and H_2O mixing ratios are somewhat different. The calculation routine is currently set up for only constant mixing ratios, whereas Kyle used a decreasing H_2O mixing ratio with height. An attempt was made to fix the $\text{CO}_2:\text{H}_2\text{O}$ ratio in the lowest level. With a CO_2 mixing ratio of 322 ppm (volume), this gave a $\text{H}_2\text{O} = 1080$ ppm (volume). Also, it was found that SNIDER will not work with a zenith angle of 0° . In spite of these differences the spectra show good agreement, indicating the two routines are consistent.

In the next chapter, the spectrum calculation routine is used in a brief study that illustrates some information analysis techniques for experimental design.

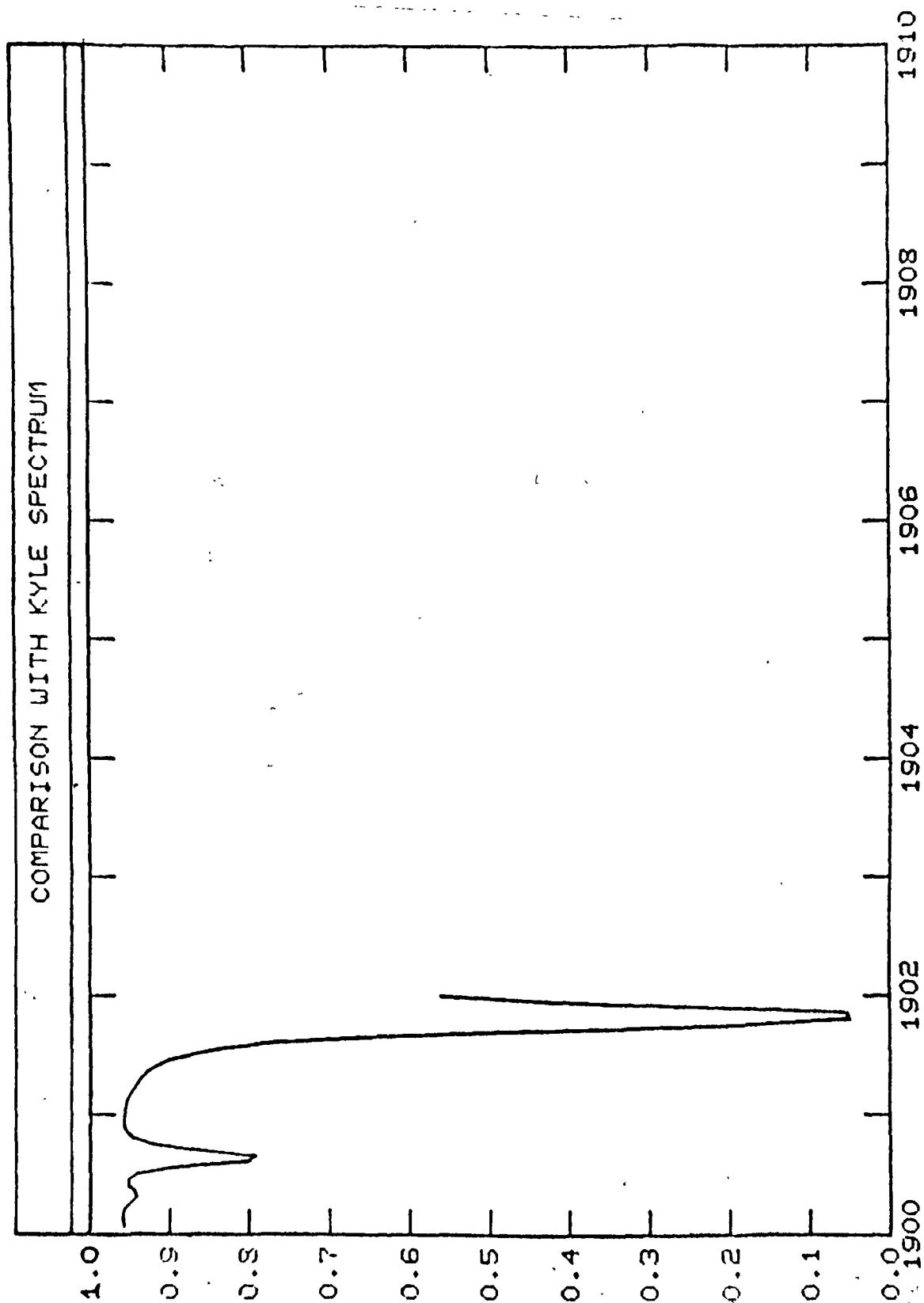


Fig. 4 - Comparison with Kyle²⁵ spectrum

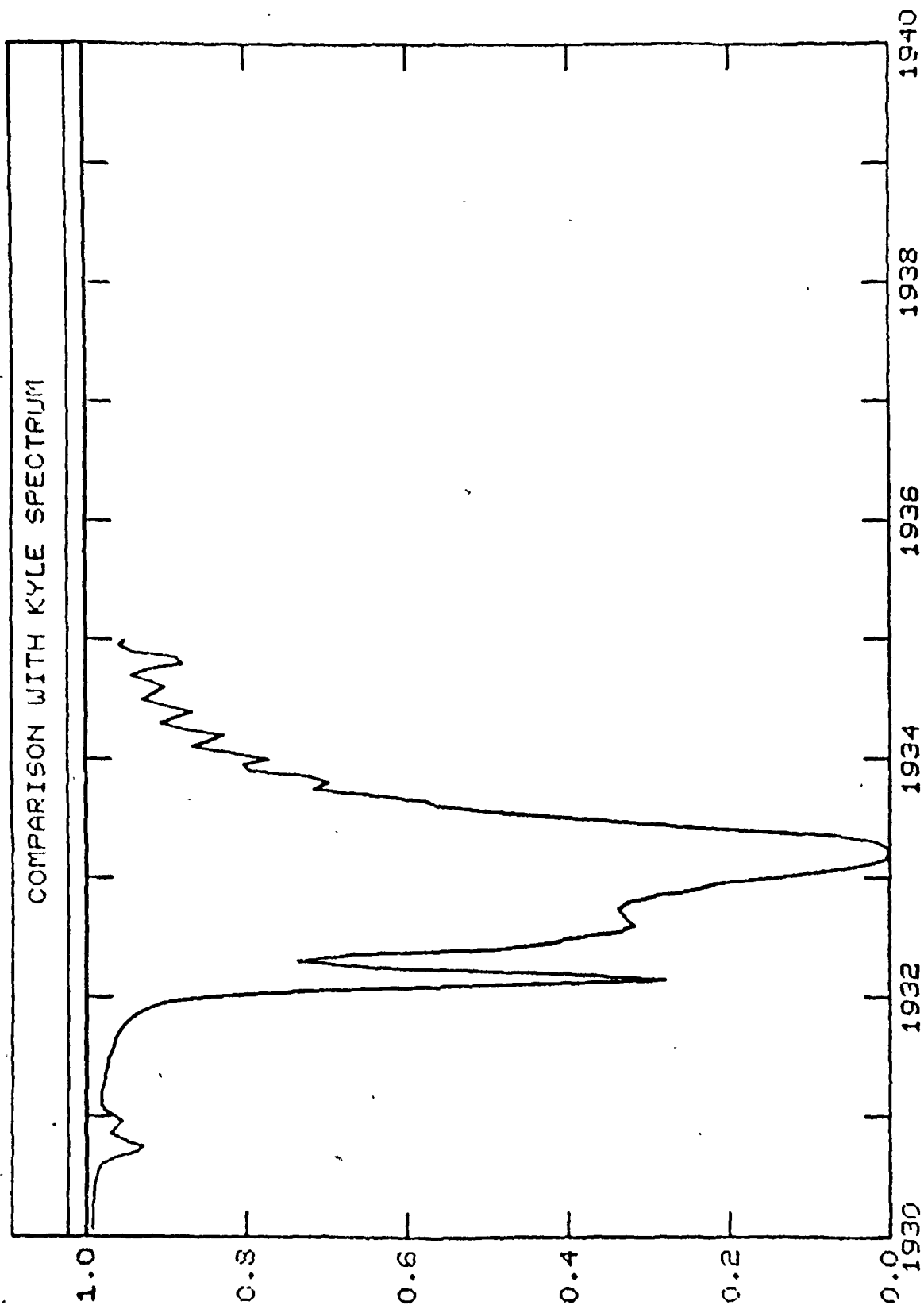


Fig. 5 - Comparison with Kyle²⁵ spectrum

III. SOME INFORMATION ANALYSIS TECHNIQUES

A. IDENTIFYING "BAD" PARAMETERS

The equations in the previous chapter describe how the appearance of an atmospheric absorption spectrum depends on the physical characteristics of the atmosphere and the molecular properties of the absorbing gases. Assuming that the molecular parameters (line intensity, broadening coefficient, line position, lower state term value) are known, the equations predict what the spectrum will look like, given the atmospheric conditions. This report is concerned with the inverse problem (i.e., inferring the atmospheric conditions given the spectrum). It is clear that those aspects of the atmosphere which have no effect on the spectrum can not be determined from the spectrum. Similarly, those aspects which have only a slight influence on the spectrum will be harder to determine than those aspects with a large influence. For example, consider the calculated spectrum in Fig. 6. This 200-point spectrum corresponds to the same observer-source geometry as in Chapter II-F with the 190-layer model and Nge equal to 15 in Eq. (25). The CO₂ mixing ratio was 322 ppm, and the H₂O mixing ratio was 3.889 ppm. Both were assumed independent of height. The slit function was Gaussian, with a full width at half height of 0.02 cm⁻¹. This particular region contains contributions from nearly 150 CO₂ lines and about a dozen H₂O lines, so it should be sensitive to the mixing ratios of CO₂ and H₂O. It contains no information, however, about the O₃ mixing ratio. A convergence criterion of 0.5% was used with an extent of 0.05 cm⁻¹ in the convolution. A more stringent criterion of 0.1% produced an rms change in the transmittance values of 2.89×10^{-4} with a maximum of 0.003, indicating that the accuracy of the convolution is consistent with the convergence criterion. A frequency spacing of 2 points per full width at half height of the slit function was used.

Several atmospheric parameters were selected for investigation. These are listed in Table 9 along with the two different values used to study the influence of the parameter on the spectrum. The spectrum in Fig. 6 corresponds to the upper value for each parameter and is referred to as the reference spectrum. Eight new spectra were then calculated by changing the values of the parameters one at a time. Figure 7 shows the effect on the spectrum of increasing the zenith angle from 95.2° to 95.4°. The difference spectrum is shown in Fig. 8. The sum of the squares of the differences for this pair is 0.44482, which is listed in column 3 of Table 9. The corresponding values are also shown for the other seven parameters. These numbers are one indicator of how much influence a particular parameter has on the spectrum. Of course larger parameter changes produce larger squared differences so the only valid comparisons between parameters are conditioned on specific parameter changes; e.g., a 0.2° change in zenith angle is more influential than a 2 K change in the temperature at layer 41 (18.38 - 18.80 km). It is reasonable, therefore, to scale the difference spectrum by dividing it by the size of the parameter change or step before squaring. Let θ_i denote the i th parameter with step $\Delta\theta_i$. The procedure above produces a set of 8 quantities W_{ii} , $i = 1, \dots, 8$

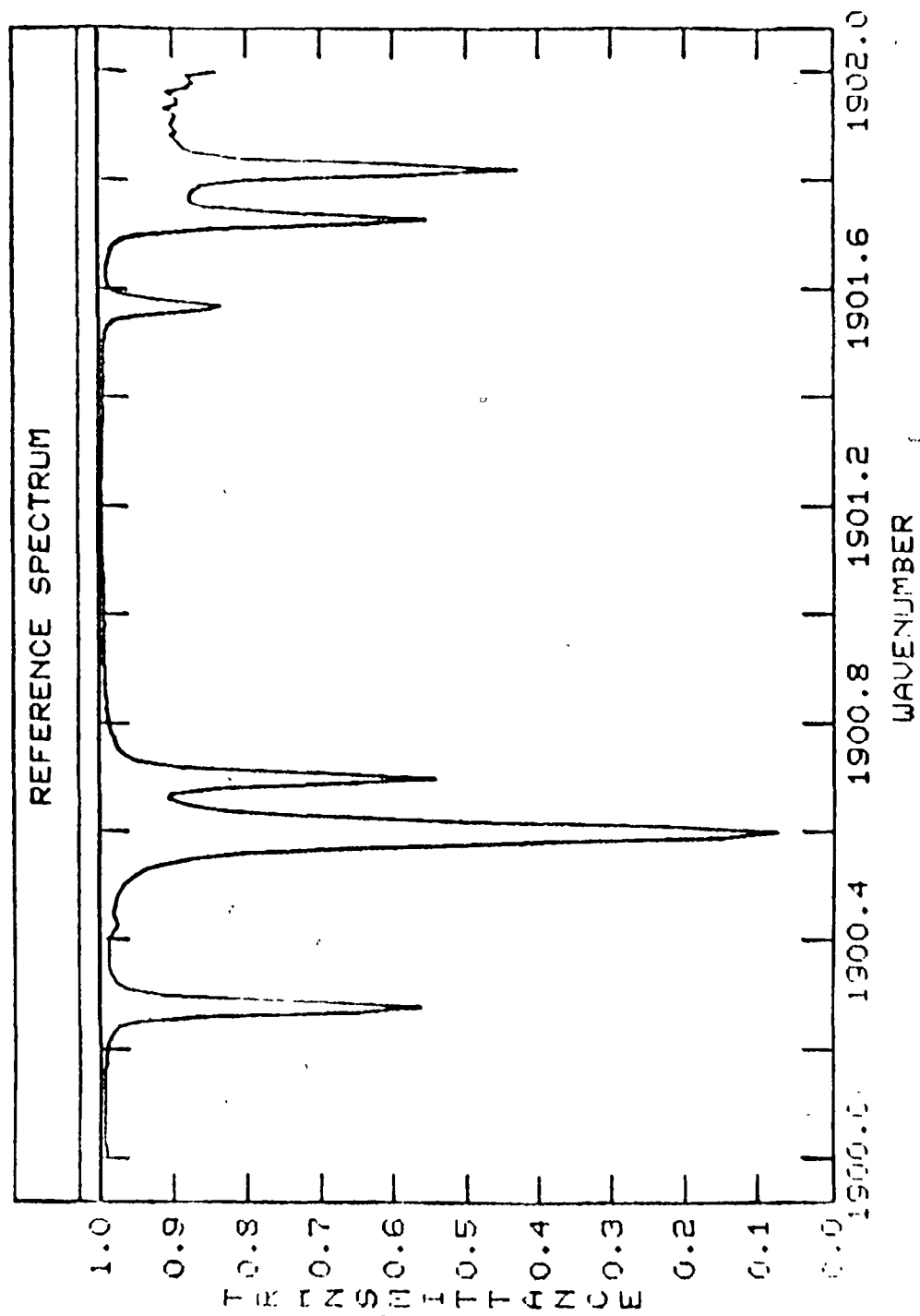


Fig. 6 - Reference spectrum

Table 9. Parameter values used to compute sample spectra.

Parameter	Values	$\sum (\Delta y)^2$
1. CO ₂ mixing ratio	322 ppm 354.2 ppm	0.011773
2. Resolution	0.02 cm ⁻¹ 0.028 cm ⁻¹	0.062913
3. Zenith angle	95.2° 95.4°	0.44482
4. Temperature in layer 41	216.65 K 218.65 K	8.4118×10^{-5}
5. Temperature in layer 42	216.65 K 218.65 K	5.4798×10^{-5}
6. Temperature in layer 40	216.65 K 218.65 K	4.888×10^{-7}
7. Ground-level pressure	1013 mb 1063 mb	0.008109
8. Background value	1.0 1.025	0.10954

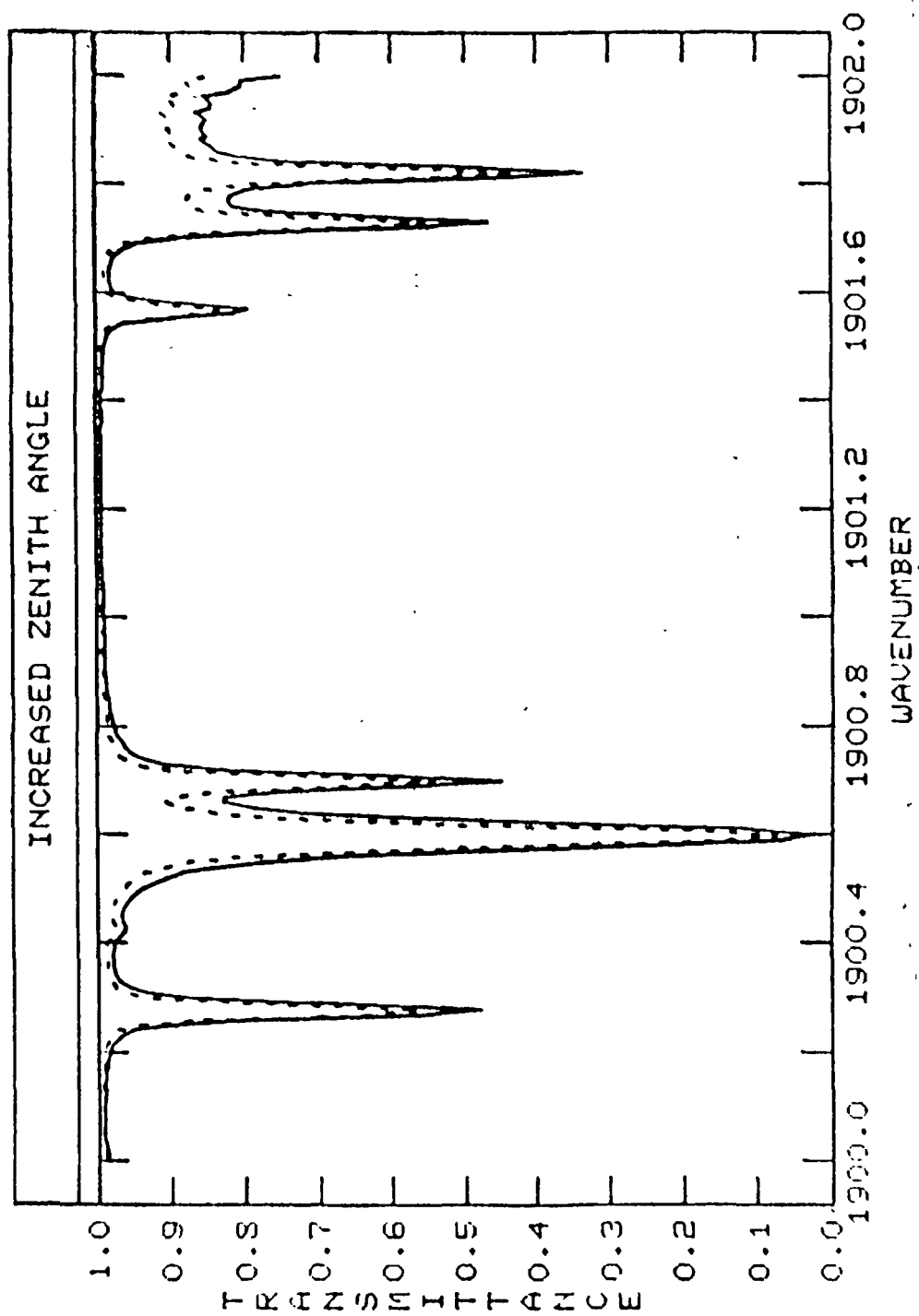


Fig. 7 - Spectrum for increased zenith angle — 95.4°, ---- 95.2° (reference spectrum)

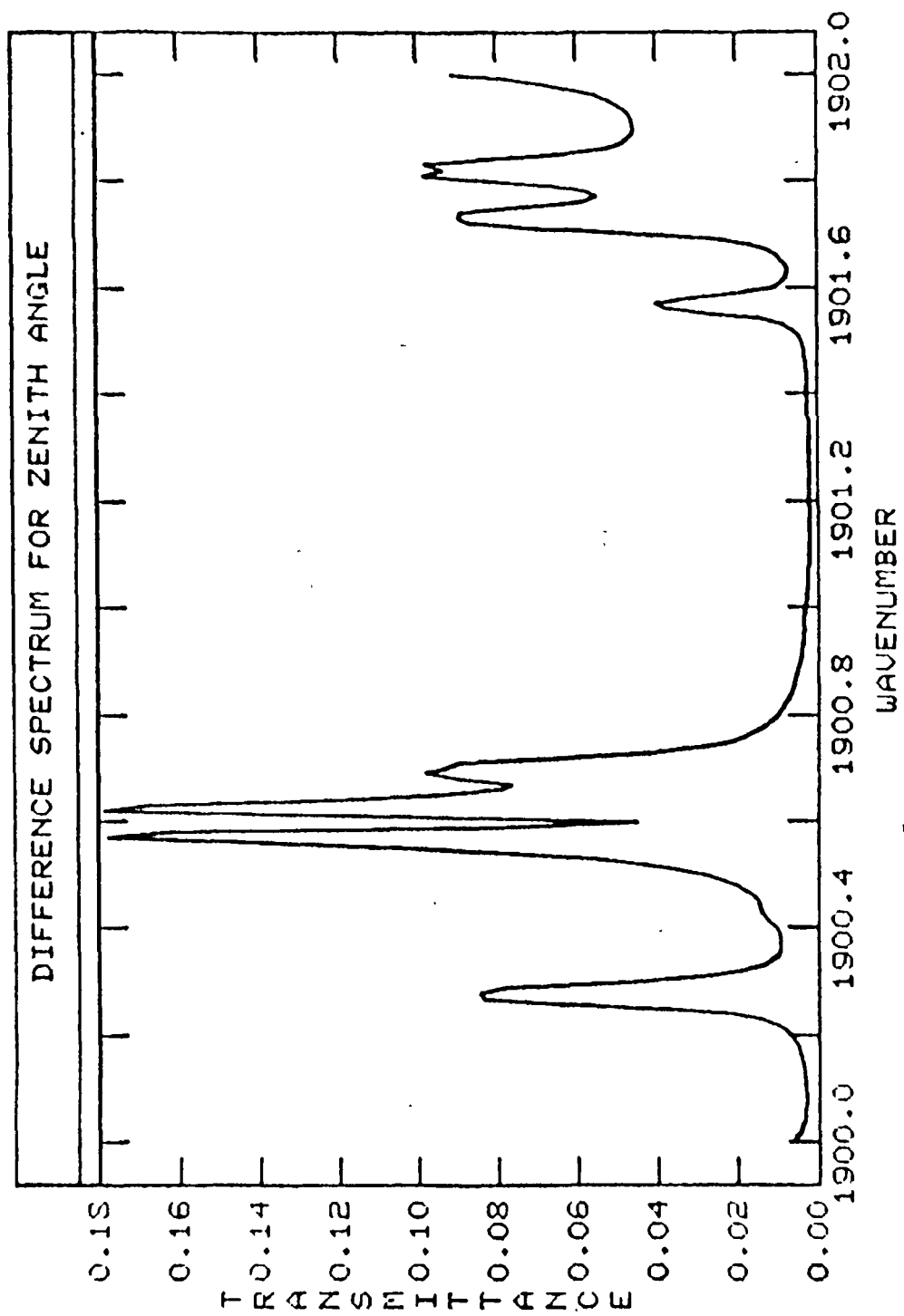


Fig. 8. (Reference spectrum) (increased zenith angle spectrum)

where

$$W_{ii} \equiv \sum_{j=1}^N \left(y_j^{(0)} - y_j^{(i)} \right)^2 / \Delta\theta_i^2, \quad (27)$$

with N the number of points in the spectrum, $\vec{y}^{(0)} = (y_1^{(0)}, \dots, y_N^{(0)})$ the reference spectrum, and $\vec{y}^{(i)} = (y_1^{(i)}, \dots, y_N^{(i)})$ the spectrum with the i th parameter stepped by $\Delta\theta_i$.

These scaled and summed square difference values alone, however, are insufficient to indicate how well groups of parameters can be determined simultaneously. This is illustrated by Fig. 9. It shows the difference spectra for changes in the temperature values $T(41)$ and $T(42)$ for layers 41 and 42. From the similarity of these spectra and the assumption that the change in the spectrum Δy is linear in $\Delta\theta$, it is clear that a simultaneous increase of 2 K in $T(41)$ and a 2 K decrease in $T(42)$ will produce a much smaller difference spectrum than either one in Fig. 9. Each change tends to cancel out the other. This corresponds to a 2 K change in $[T(41) - T(42)]/2$, with the average temperature $[T(41) + T(42)]/2$ held constant. Similarly, a simultaneous 2 K increase in $T(41)$ and $T(42)$ will produce a much larger difference spectrum than either in Fig. 9. This corresponds to a 2 K change in the average temperature, with the difference temperature held constant, and indicates that changes in different linear combinations of the parameters can have significantly different amounts of influence on the spectrum. That, in turn, implies that some combinations are harder to determine from a spectrum than others. Similar observations apply to linear combinations of all 8 different parameters.

The question arises as to whether there exists some linear combination

$$\phi = \sum_{j=1}^8 w_j \theta_j$$

which has the least influence on the spectrum and hence is the hardest to determine. Lees²⁶ addressed this question in connection with attempts to analyze methyl alcohol spectra. He found that changes in a particular linear combination of the unknown parameters produced no change in the spectrum, which he called a linear dependence, and he proposed a technique for identifying these as well as "near" linear dependences. In order to adapt this technique to the present problem, form the quantities

$$W_{ik} = \sum_{j=1}^N \left(y_j^{(0)} - y_j^{(i)} \right) \cdot \left(y_j^{(0)} - y_j^{(k)} \right) / \Delta\theta_i \Delta\theta_k \quad (28)$$

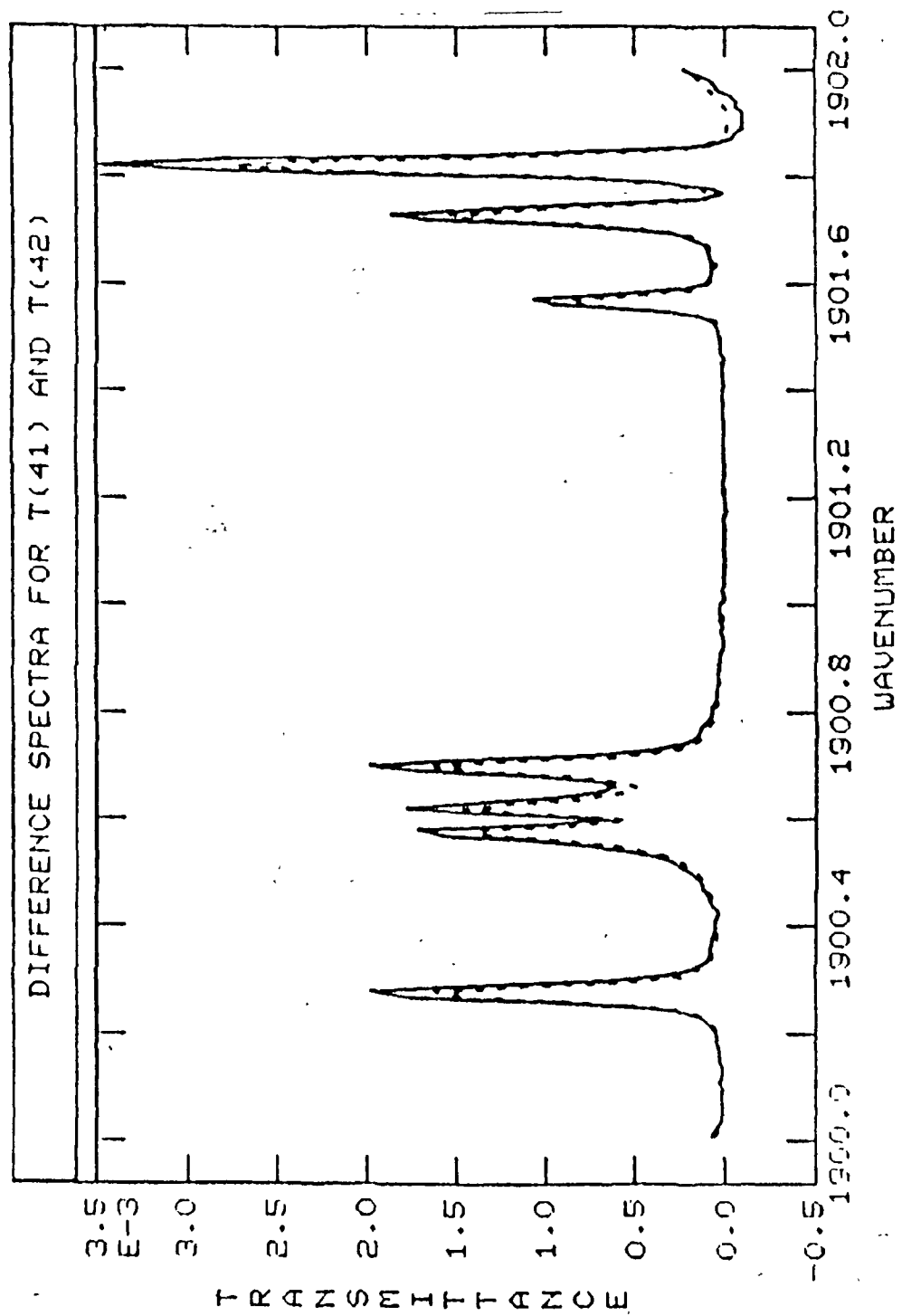


Fig. 9 - Difference spectra for 2 K changes in the temperature in layers 41 and 42. — $\Delta T(41) = 2$ K, $\Delta T(42) = 0$, ---- $\Delta T(41) = 0$, $\Delta T(42) = 2$ K.

and place these in a matrix W , where the i th diagonal element is W_{ii} from Eq. (27) and the i - k th and k - i th element is W_{ik} . This matrix is often referred to as the information matrix²⁷ or the curvature matrix.²⁸

To be more precise, W becomes the information matrix in the limit as $\Delta\theta \rightarrow 0$ and the quantities $y^{(0)} - y^{(i)}/\Delta\theta^i$ become the partial derivative of y with respect to θ_i evaluated at $\vec{\theta}_0$. W is therefore a function of $\vec{\theta}_0$.

For small simultaneous changes in the parameters $\vec{\Delta\theta} = \begin{pmatrix} \Delta\theta_1 \\ \vdots \\ \Delta\theta_8 \end{pmatrix}$ the summed squared difference spectrum is given by

$$Q(\vec{\Delta\theta}) = \sum_{ij} \Delta\theta_i W_{ij} \Delta\theta_j = \sum_k \left[y_k^{(0)} - y_k(\vec{\Delta\theta}) \right]^2 \quad (29)$$

or, in matrix notation,

$$Q(\vec{\Delta\theta}) = \vec{\Delta\theta}' W \vec{\Delta\theta} ,$$

where ' denotes transpose. Lees proposes examining the eigenvalues and eigenvectors of a modified information matrix W^* given by

$$W_{ik}^* = W_{ik} / \sqrt{W_{ii} W_{kk}} .$$

Let the eigenvector $\vec{\lambda}^*$ with elements λ_i^* correspond to the smallest eigenvalue of W^* . The corresponding linear combination of parameters is given by

$$\phi = \sum_{j=1}^8 \lambda_j^* \cdot \theta_j \cdot \sqrt{W_{jj}} . \quad (30)$$

When this eigenvalue is much smaller than the others, he says that it indicates a "near" or exact linear dependence. Table 10 lists the information matrix W , and modified matrix W^* for the set of 9 spectra already introduced. The eigenvalues and eigenvectors of W^* were calculated in SPEAKEASY with the command EIGENVALS. These are listed in Table 11. None of the eigenvalues is significantly lower than the rest, indicating that there are no exact linear dependences among the 8 parameters in Table 9. It is still possible to deduce the "worst" linear combination from these results with the following restriction:

For each of the 8 parameters θ_i define a parameter step $\Delta\theta_i$ such that $Q(\Delta\theta_i) = 1$. Assuming that Eq. (29) holds, these steps are given by $\Delta\theta_i = 1/\sqrt{W_{ii}}$. The appropriate steps are listed in Table 12. Define new parameters $\{\psi\}$ according to

$$\psi_i \equiv \theta_i / \Delta\theta_i .$$

Table 10. Information matrices

W:		W*:					
ROW 1	1.1355E-5 1.0832E-6	0.034772 5.7883E-6	0.010634 -0.020427	1.2303E-5	1.0215E-5		
ROW 2	0.034772 -1.8376E-4	3932 -0.0091847	-1.6132 -70.879	-0.090516	-0.072398		
ROW 3	0.010634 0.0011462	-1.6132 0.0059693	11.12 -22.043	0.012685	0.010461		
ROW 4	1.2303E-5 1.3054E-6	-0.090516 7.0995E-6	0.012685 -0.021157	2.1029E-5	1.6957E-5		
ROW 5	1.0215E-5 1.0741E-6	-0.072398 5.8427E-6	0.010461 -0.017702	1.6957E-5	1.3699E-5		
ROW 6	1.0832E-6 1.222E-7	-1.8376E-4 6.2136E-7	0.0011462 -0.0020892	1.3054E-6	1.0741E-6		
ROW 7	5.7883E-6 6.2136E-7	-0.0091847 3.2436E-6	0.0059693 -0.011075	7.0995E-6	5.8427E-6		
ROW 8	-0.020427 -0.0020892	-70.879 -0.011075	-22.043 175.27	-0.021157	-0.017702		
W*:							
1	-0.165	0.946	0.796	0.819	0.920	0.954	-0.458
	1	-0.0077	-0.315	-0.312	-0.0084	-0.081	-0.085
		1	0.829	0.848	0.983	0.994	-0.499
			1	0.999	0.814	0.860	-0.348
				1	0.830	0.876	-0.361
[SYMMETRIC]					1	0.987	-0.451
						1	-0.465
							1

Table 11. Eigenvalues and associated eigenvectors of W^* from Table 10.

Eigenvectors of W^* (as columns):					
ROW 1	-0.02216 -0.043359	0.069408 0.015821	-0.25559 -0.39562	0.74657	0.46191
ROW 2	0.0038524 -0.39618	-0.032105 0.83294	-0.052676 0.06913	0.18343	-0.32712
ROW 3	-0.008285 -0.11331	0.48954 0.14197	0.71662 -0.40684	-0.13348	0.17436
ROW 4	-0.67639 -0.048948	0.08705 -0.23103	-0.093432 -0.38268	0.087113	-0.56248
ROW 5	0.7281 -0.045501	-0.032767 -0.21962	-0.0074687 -0.38829	0.12842	-0.50117
ROW 6	0.062616 -0.17077	0.23679 0.13061	-0.59867 -0.40051	-0.57696	0.20514
ROW 7	-0.088656 -0.1211	-0.83043 0.068128	0.22346 -0.41116	-0.18346	0.17485
ROW 8	4.4771E-4 -0.88319	0.013133 -0.40311	0.034914 0.21564	0.023464	0.095041

Eigenvalues of W^* :

- (1) 1.0655×10^{-4}
- (2) 0.0016232
- (3) 0.010273
- (4) 0.064734
- (5) 0.29085
- (6) 0.68626
- (7) 1.1985
- (8) 5.7477

Table 12. Parameter steps producing a summed squared difference spectrum equal to 1, assuming Eq. (29) holds.

(1)	296.76 ppm (CO_2 mixing ratio)
(2)	0.015948 cm^{-1} (resolution)
(3)	0.29988° (zenith angle)
(4)	218.07 K $\Delta T(41)$
(5)	270.18 K $\Delta T(42)$
(6)	2860.6 K $\Delta T(40)$
(7)	555.25 mb $\Delta P(0)$
(8)	0.075535 (background)

For these new parameters, a unit step in ψ_i produces a $Q(\Delta\psi) = 1$. Now consider the set of all linear combinations of steps in the $\{\psi\}$ of the form

$$\vec{\Delta\phi} = \begin{pmatrix} c_1 \Delta\psi_1 \\ c_2 \Delta\psi_2 \\ \vdots \\ c_8 \Delta\psi_8 \end{pmatrix}$$

such that

$$\sum_k c_i^2 = 1. \quad (31)$$

The set of steps $\vec{\Delta\phi}_i$, with

$$c_i = 1$$

and

$$c_j = 0; \quad i \neq j,$$

belongs to this set of $\vec{\Delta\phi}$ satisfying Eq. (31), and for each $\vec{\Delta\phi}_i$, $Q(\vec{\Delta\phi}_i) = 1$. In a sense, steps $\vec{\Delta\phi}$ satisfying Eq. (31) are all the steps of the same "size," in terms of parameter changes. From the theorems on quadratic forms²⁹ it can be shown that the extremal values of $Q(\vec{\Delta\phi})$ for all $\vec{\Delta\phi}$ correspond to $\vec{\Delta\phi}$'s whose $\{c_i\}$ values are the elements of the eigenvalues of W^* . Consequently the smallest $Q(\vec{\Delta\phi})$, and hence smallest change in the spectrum, for all parameter changes of the same "size" as those in Table 12 results from:

$$\vec{\Delta\phi}_{\min} = \begin{pmatrix} -0.02216 & \times & 296.76 \text{ ppm} \\ 0.0038524 & \times & 0.015948 \text{ cm}^{-1} \\ -0.008285 & \times & 0.29988^\circ \\ -0.67639 & \times & 218.07 \text{ K} \\ 0.7281 & \times & 270.18 \text{ K} \\ 0.062616 & \times & 2860.6 \text{ K} \\ -0.088656 & \times & 555.25 \text{ mb} \\ 4.4771 \times 10^{-4} & \times & 0.075535 \end{pmatrix}$$

$$= \begin{pmatrix} -6.576 \text{ ppm} \\ 0.00006144 \text{ cm}^{-1} \\ -0.0024845^\circ \\ -147.5 \text{ K} \\ 196.7 \text{ K} \\ 179.1 \text{ K} \\ -49.23 \text{ mb} \\ 3.382 \times 10^{-5} \end{pmatrix}.$$

The most significant aspect of this set of parameter changes is the temperature steps. The temperature in level 41 is decreased by 147.5 K while the temperatures in the two adjacent layers are increased by approximately the same amount. This zigzagging of the temperature profile is a problem that often occurs in profile retrievals.³⁰ The summed squared difference spectrum corresponding to this "worst" set of parameter changes is given by the corresponding eigenvalue from Table 11; i.e., 1.0655×10^{-4} . It is seen that this is smaller than most of the values in the third column of Table 9.

The same quadratic forms theorem allows the identification of the set of parameter changes $\vec{\Delta\phi}_{\max}$ leading to the largest change in the spectrum. It is given by the eigenvector associated with the largest eigenvalue of W^* . From the eighth column in Table 12 it is seen that $\vec{\Delta\phi}_{\max}$ corresponds to simultaneous decreases in CO₂ mixing ratio, zenith angle, ground level pressure, and all three temperature values. All of these changes tend to decrease the amount of absorption in the spectrum and hence add together to increase the summed squared difference spectrum. The net change in the spectrum is more than 50,000 times larger than for $\vec{\Delta\phi}_{\min}$.

B. ESTIMATED PARAMETER UNCERTAINTIES

Another useful property of the information matrix W is related to the uncertainties in estimates for the values of the unknown parameters to be determined from an observed spectrum \vec{y}_{obs} . If $\vec{y}(\vec{\theta})$ is the calculated

spectrum for the set of parameter values $\hat{\theta}$, then one estimate for the true parameter values corresponding to \bar{y}_{obs} is the well-known least-squares estimate $\hat{\theta}$. This is given by the value of $\hat{\theta}$ which minimizes

$$\sum_{i=1}^N [y_{\text{obs},i} - y(\hat{\theta})_i]^2 .$$

If the rms noise value is σ , then the asymptotic variance-covariance matrix for $\hat{\theta}$ is

$$\hat{S} = \sigma^2 W^{-1} ,$$

where W is evaluated at $\hat{\theta}$.

The matrix in Table 10 can therefore be used to estimate, for a given noise level, how precisely the eight parameters in Table 9 could be obtained from a spectrum similar to that in Fig. 6. Attempts to invert W , however, led to warnings by the inversion routine that the matrix is nearly singular and the calculated inverse may not be significant. This implies that numerical difficulties would be encountered while trying to retrieve all eight parameters. If several of the parameters are constrained to given values, this eliminates the corresponding row and column from W . In general this makes retrieval of the other parameters easier. The effect of various sets of constrained parameters were studied by eliminating selected rows and columns and then trying to invert the resulting reduced matrix. Some of the results obtained are listed in Table 13. It is seen from the column labeled 3, that if only the CO_2 mixing ratio, resolution, and zenith angle are determined from a spectrum like Fig. 6 with 1% noise, the respective uncertainties are 10.5 ppm, 0.00018 cm^{-1} , and 0.0105°. If the noise is 2%, the uncertainties would be twice as large. Any attempts to determine more than one temperature value always led to very large uncertainties, as compared to the cases where only one temperature was determined. This is consistent with the conclusions in the previous section. Trying to determine $T(41)$ and $T(42)$ is the same as trying to determine their difference and average. Yet the temperature difference is very hard to determine, and this gives rise to increased uncertainties in $T(41)$ and $T(42)$.

Another way to think of this problem is to consider the addition of a constraint as an injection of information into the analysis. The additional information spreads out over the variance-covariance matrix and leads to smaller uncertainties in the unconstrained parameters. The extent to which the constraint of θ_i improves the retrieval of θ_j is determined by the correlation coefficient between θ_i and θ_j . This is given by $S_{ij}/\sqrt{S_{ii}S_{jj}}$.

It is also seen in Table 13 that attempts to retrieve the zenith angle and the ground level pressure $P(0)$ produced inversion problems and increased uncertainties. From Table 11 it is seen that this corresponds to the second "worst" parameter combination (column 2 of eigenvectors). Its

Table 13. Parameter uncertainties for various sets of parameter constraints, assuming an rms noise of 1%.

Parameter	1	3	6	7	8	9
1 CO ₂ mix. r.	14.2* ppm	10.5	10.97	10.87	10.87*	10.54*
2 resolution	0.00026* cm ⁻¹	0.00018	0.00023	0.00023	0.00018*	0.00023*
3 zenith angle	0.042°*	0.0105	0.0137	0.0138	0.023*	0.040*
4 T(41)	119.5 K*	-	4.91	-	-	-
5 T(42)	157.1 K*	-	-	6.47	-	-
6 T(40)	-	-	-	-	166.2 K*	-
7 P(0)	78.4 mb*	-	-	-	-	72.8*
8 background	0.00094*	-	0.00088	0.00088	0.00091*	0.00094*

*indicates inversion of nearly singular matrix

corresponding eigenvalue, though larger than the smallest, is still 5,000 times smaller than the largest eigenvalue and therefore corresponds to a set of parameter steps having a small effect on the spectrum.

The above techniques of information analysis explore the quality of the information in a proposed set of data. They can be used, therefore, to compare different experimental designs by comparisons of the information in the data produced by the different designs. This function of the techniques was employed to study the effect of decreased instrument resolution on the information in the spectra analyzed above.

C. LOW RESOLUTION INFORMATION ANALYSIS

The calculation steps of the previous two sections were repeated with the parameter values in Table 14. The new reference spectrum is shown in Fig. 10. This spectrum contains 40 points from 1900 - 1902 cm^{-1} which is 2 points per full width at half height of the slit function. Clearly, since there are five times more points in the high-resolution spectra, the summed squared difference spectra should be correspondingly higher. Any deviation from a five-fold change is an indication of differences in the influence of the parameters on the spectrum. The ratios of the summed squared difference spectra are listed in column 4 of Table 14. Only the value for the resolution is less than the expected value of 5. Since both resolution changes were +4%, this implies that the low-resolution spectrum is more sensitive to percent changes in instrument resolution than the high-resolution spectrum. Similarly, the large value (9.23) for $T(41)$ indicates that the low-resolution spectrum is less sensitive to changes in the temperature in layer 41 and hence should yield considerably larger uncertainties in this parameter. Table 15 shows some typical standard deviations for the low-resolution spectrum. It is seen that the uncertainties are larger than for the high-resolution spectrum, especially the temperature uncertainties.

Table 16 shows some of the results of a Lees-type search for the "bad" parameters. The lowest eigenvalue of the modified information matrix corresponds to the zenith angle and $P(0)$ values and the second lowest corresponds to the zigzagging temperature values. This is a reverse in order from the high-resolution case for the two "worst" combinations. Once again, however, the best combination is a simultaneous decrease in CO_2 mixing ratio, zenith angle, ground-level pressure, and all three temperatures. The variation from worst to best corresponds to a change in summed squared difference of better than 100,000.

Table 14. Parameter values used to calculate low-resolution sample spectra. (The fourth column gives the ratio of the $\sum (\Delta y)^2$ values from Table 9 and those in column 3 for each parameter.)

Parameter	Values	$\sum (\Delta y)^2$	Ratio of $\sum (\Delta y)^2$
(1) CO ₂ mixing ratio	322 ppm 354.2 ppm	0.0016442	7.16
(2) Resolution	0.10 cm ⁻¹ 0.14 cm ⁻¹	0.014764	4.26
(3) Zenith angle	95.2° 95.4°	0.070241	6.33
(4) Temperature in layer 41	216.65 K 218.65 K	9.1177 × 10 ⁻⁶	9.23
(5) Temperature in layer 42	216.65 K 218.65 K	6.147 × 10 ⁻⁶	8.91
(6) Temperature in layer 40	216.65 K 218.65 K	7.6 × 10 ⁻⁸	6.43
(7) Ground-level pressure	1013 mb 1063 mb	0.0012427	6.53
(8) Background value	1.0 1.025	0.021652	5.06

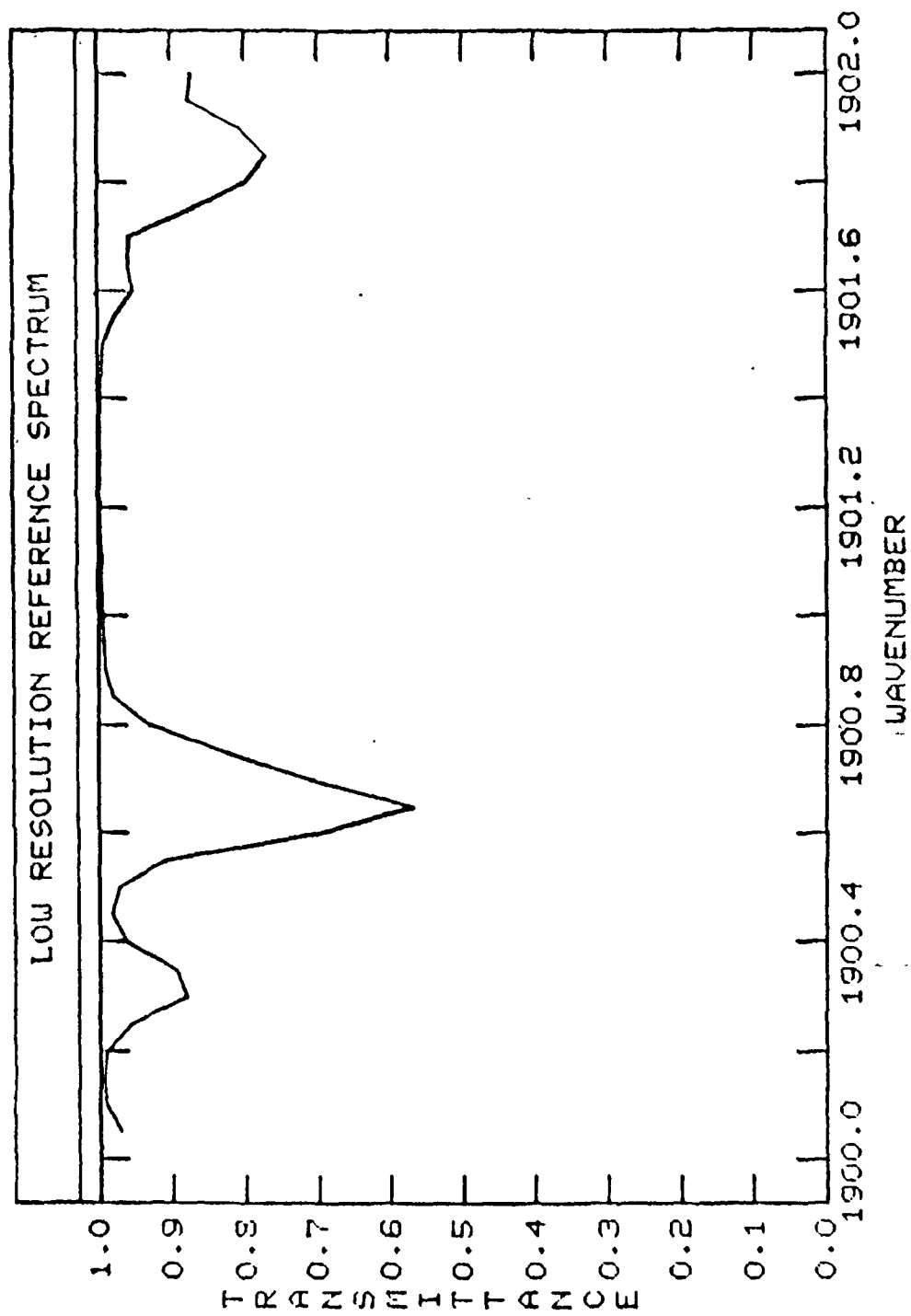


Fig. 10 - Low-resolution reference spectrum

Table 15. Parameter uncertainties for various sets of parameter constraints for low-resolution spectra, assuming an rms noise of 1%.

Parameter	2	3	6	7	8	9
1 CO ₂ mix. r.	61.01 ppm	60.43	61.54	61.93	63.41	64.02*
2 resolution	0.0036 cm ⁻¹	0.0034	0.0042	0.0041	0.0038	0.012*
3 zenith angle	0.057°	0.057	0.059	0.059	0.092	0.702*
4 T(41)	-	-	23.03 K	-		
5 T(42)	-	-	-	29.97 K		
6 T(40)	-	-	-	-	531.3 K	
7 P(O)	-	-	-	-		1286* mb
8 background	0.0022	-	0.0023	0.0023	0.0023	0.0027*

*indicates inversion of nearly singular matrix

Table 16. Some eigenvectors and associated eigenvalues of modified information matrix for low-resolution spectra.

Eigenvectors:			
(1)	(2)	• • •	(8)
0.0083607	0.05296		-0.3934
0.025936	0.0074088		0.11675
-0.70477	-0.13512		-0.39486
-0.16379	0.65338		-0.38916
-0.17926	-0.70975		-0.39096
-0.016959	-0.06559		-0.38969
0.66577	0.20956		-0.39544
-0.0071575	0.0028461		0.25133
Eigenvalues:			
(1)	5.3967×10^{-5}		
(2)	1.4169×10^{-4}		
(3)	0.0062167		
(4)	0.020332		
(5)	0.12136		
(6)	0.45162		
(7)	1.134		
(8)	6.2663		

IV. CONCLUSIONS

This report has described the operation of a computer program for calculating atmospheric absorption spectra for slant paths through the atmosphere, using as input the AFGL line parameter listing. This program, unlike many others, was specifically written to employ an efficient means of including the effects of instrument spectral response functions. In addition the routine is written so that the precision of the convolved or degraded spectral values can be varied to match the noise level of observed spectra. The program was tested and compared to calculated spectra from another source and found to be working correctly.

Some information analysis techniques were then applied to a particular example of slant path spectra. The analysis included an identification of the "bad" parameters and estimated uncertainties for possible sets of unknown parameters. All that was required was a set of spectra and the corresponding conditions for each spectrum. With the aid of a few simple matrix operations the character of the information in the spectra was quickly determined. These techniques are simple and versatile and could be used on many different types of data, both simulated (as in this study) or observed.

The analysis indicated that trying to retrieve closely spaced temperature profile values can lead to large uncertainties in the temperature difference. Problems were also found with simultaneous retrieval of the base level pressure and apparent zenith angle. By analyzing a second set of spectra at a lower spectral resolution, the loss of information with loss of resolution was investigated. In particular, the loss of temperature information was found to be more pronounced than that for the other spectral parameters considered.

Blank Page
48

APPENDIX A

THE SPECTRUM CALCULATION PROGRAM

The basic layout of the program is shown in the flow chart (Fig. A-1). The four basic parts are (1) a main program controlling input and output and calculation order; (2) the Snider-Goldman slant path program (subroutine SNIDER and associated subroutines called within SNIDER) for calculating the path of radiation in an inhomogeneous atmosphere; (3) subroutine PATHST for converting the output of SNIDER into a series of layers with specific airmass, temperature, and pressure values; and (4) subroutine NSPEC for calculating the spectrum. All of the source statements for these parts are listed at the end of this appendix.

I. MAIN PROGRAM

There are three basic sets of inputs needed by the main or controlling program; these are listed in Table A-1. The first consists of the input parameters for the Snider-Goldman routine; these specify the observer-source geometry (ALAT, Z, HOBS) and the atmospheric profile (LEVELS, H, T, P). Since SNIDER produces its own pressure profile by integrating the hydrostatic equation and using $P(0)$ and the temperature profile, only the first pressure value is used.

The second set consists of parameters needed by PATHST. These are a value for N_{ge} , which determines the smallest airmass in a layer of [total airmass/ N_{ge}], and a set of values, $R(1)$, $R(2)$, . . . , $R(5)$, for calculating the mixing ratios in the layers. As currently written, only constant mixing ratios are allowed, but other types can be easily included by suitably modifying subroutine RMIX. Also, provision has been made for only five absorbing species but others could be included.

The third set of inputs are values needed to control NSPEC. These include the upper and lower frequency positions, VU and VL; the number of observed frequency values, NVO; and the parameters which control the convolution routine. These latter are discussed more fully in Chapter III describing subroutine NSPEC. Also included in this set is the unit number for the line parameters. This parameter must be passed to NSPEC which controls the input of the line parameter data for the spectrum calculation.

The output from the main program is in two parts. First is the calculated transmittance values starting from $\tau(VL)$ up to $\tau(VU)$. Second is a series of error codes. The subroutine ERROR called in the last statement of the controlling program dumps the stored error code numbers for any errors which may have occurred during execution of previous steps. These code numbers are in the order in which the errors occurred, and may be interpreted by referring to Table A2. No claims for completeness are made for this list of errors. An attempt was made to write self-correcting routines into the program for some of the more simple errors, but there are undoubtedly many which have not been corrected for. The first output

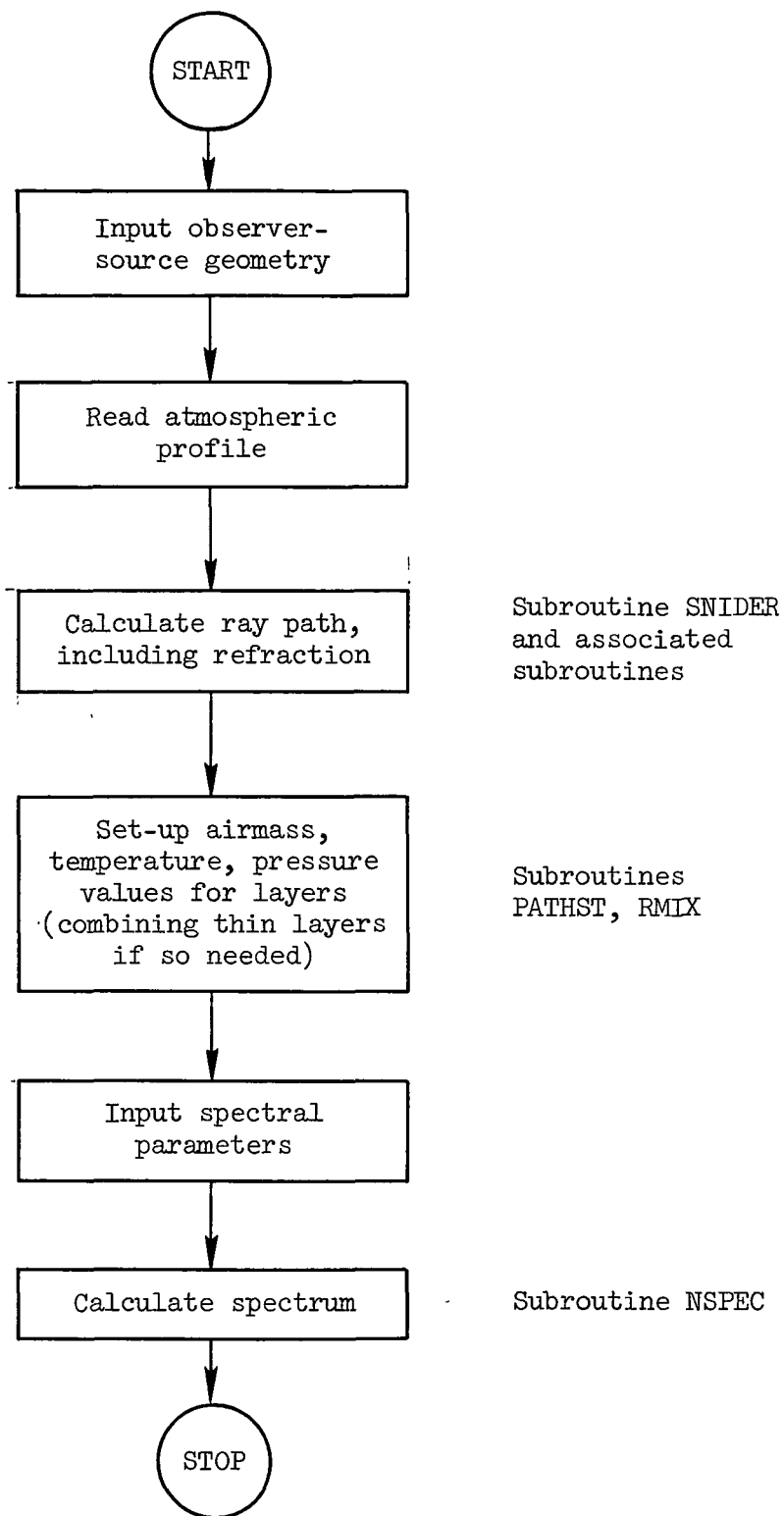


Fig. A1 - Overall program logic.

Table A1. Inputs to main program.

LEVELS	Number of levels in atmospheric profile (must be less than 190)
ALAT	Latitude of the observer (in degrees)
Z	Apparent zenith angle of incoming ray (in degrees)
HOBS	Observer height (in kilometers)
NGE	Integer for structuring layers for input to spectrum calculation routine
LUNIT	Unit number of file containing line parameters. This must be the same number as in a JCL DD card; e.g., if LUNIT = 11 then there is a DD card of the form //GO.FTLLFOOL DD . . . identifying the line parameter file.
H, T, P	Atmospheric profile where H is the height in kilometers, T is the temperature in Kelvin, and P is the pressure in mb. These are on unit 10 (see above).
R	An array of mixing ratio values. As currently written it requires five values R(1), . . . , R(5) for the volume mixing ratio of each species; i.e., (molecules of absorber)/(total molecules).
VL	Lower frequency position in cm^{-1}
VU	Upper frequency position in cm^{-1}
NVO	Number of observed frequency values
NM NO	Set convolution iteration limits (see write-up for subroutine NSPEC)
EPA	Convergence criterion. This corresponds to the estimated uncertainty in the transmittance values.
EXTNT	Sets the integration limits for the convolution. It is given as the number of B values (see below) in the integral.
B	Resolution width in cm^{-1} . As currently written this value is half of the full width at half max of a Gaussian slit function.
LINTOP	Sets the maximum number of lines contributing to any one spectral value (must be less than 200)

Table A1 (continued)

TTOP	Sets the maximum value of the absorption coefficient. When a calculated absorption coefficient exceeds TTOP, the corresponding monochromatic transmittance is set to zero.
NTST	Integer debug flag used to output intermediate convolution results.
NTST = 0	normal operation
NTST = 1	the M- and T-table values are printed out on unit 13 for each step of each convolution
NTST = 2	the monochromatic transmittance values and corresponding frequency positions are printed out on unit 14
	The NTST = 2 function has been removed from the version listed in this appendix.

All input is done with unformatted READ statements so that there are no specific format requirements for the input cards.

Table A2. Error codes for subroutine ERROR.

Code No.	Description of Error and Action Taken
1	LEVELS value is greater than 190. LEVELS is set to minimum of 190 and LEVELS.
2	SNIDER could not find index of atmospheric layer containing the observer. Execution terminated.
3	SNIDER could not find index of atmospheric layer containing the source. JHT is set equal to LEVELS, where JHT is the variable labeling the index of the source layer. This is equivalent to assuming the source is at the top of the atmosphere.
4	Zenith angle is incorrect for specified observer-source geometry; e.g., $Z > 90$ but $H_{OBS} > H_{source}$. Execution terminated.
5	SNIDER has looped 10 times trying to find astronomical zenith angle without success to 0.001. Execution terminated [see Ref. (10)].
6	GAMMA = 0 in subroutine OM. Execution continues; results may be in error.
7	Error in OM, not #6 above. Execution continues; results may be in error.
8	Error in subroutine OPT1. Execution continues, results may be in error.
9	FTOT in subroutine PATHST is less than or equal to 0.001, indicating that essentially no airmass is in the path. Execution continues; results may be in error.
10	NM in subroutine NSPEC was specified too large. NM is set to minimum of 7 and NM.
11	Failure to converge in convolution routine of subroutine NSPEC for current value of frequency position and specified maximum number of iterations. Execution continues; current value on T-table main diagonal is used as transmittance value.

Table A2 (continued)

Code No.	Description of Error and Action Taken
12	NLINEs equals zero in subroutine NSPEC, indicating that there are no active lines at the current frequency position. Execution continues; transmittance value is set equal to 1.
13	The number of active lines, NLINEs, is greater than LINTOP, the capacity of array IACTV. Execution continues; enough lines are kicked out so that NLINEs equals LINTOP.
14	VU < VL. Execution terminates.

value from ERROR is the number of type 11 errors which occurred. Since this is a common error and may occur many times, only the number is kept and not the sequence. Use of NTST = 1 may be used to check specific frequency positions.

II. SUBROUTINE SNIDER

Questions about the operation of this part of the program can be answered by referring to Ref. (10). A few minor changes were made in the program listed in that reference in order to run it as a subroutine.

The most important change involved collecting all the error corrections into the error code listing (Table A-2). Also the profile input section was modified.

In addition to these changes, statements were inserted to cause SNIDER to output the individual layer parameters (T,P,u) as it traced the ray through the atmosphere. This is done by calls to subroutine POUT. The layer parameters are stored in the array UED, PED, and TED kept in blank COMMON.

An attempt was made to preserve as much of the flexibility of the Snider-Goldman program as possible. This includes the option of specifying the astronomical zenith angle and having the program find the corresponding apparent zenith angle by an iterative search. To use this facility, the input to SNIDER must be changed so that LSTOP, the 4th input value passed to SNIDER, is equal to 1; see Ref. (10) before using this option.

One minor problem encountered with SNIDER during debugging is that it will not run with an input zenith angle of zero. The associated subroutines are OM, OPT1, ASINX, ZCOMP, QUAD, GETT, and POUT.

III. SUBROUTINE PATHST

This subroutine takes the individual layer parameters stored in UED, PED, and TED and rearranges them into a set of layers with nearly the same airmass values stretching from the lowest layer crossed by the ray up to the highest level.

First it sums all the airmass values to get FTOT, the total airmass. It then folds the parameter arrays to combine contributions from the same layer that occurred during the descending and ascending portions of the path, if the zenith angle is greater than 90° . It next starts from the lowest layer and combines the contributions of the next highest layers until the summed airmass exceeds FTOT/Nge. A call to subroutine RMIX returns a set of mixing ratio values for this composite layer and then the program begins combining the next layers until the airmass again exceeds FTOT/Nge. The recombination continues throughout the entire path. The resulting modified set of atmospheric path parameters is stored in U, PRES, TMP, and RMIXR in blank COMMON.

IV. SUBROUTINE NSPEC

This subroutine takes the path parameters from PATHST, the line parameters from unit LUNIT, and the frequency and convolution parameters from the SUBROUTINE call and calculates the transmittance. The file of line parameters has been created by a separate program BOB listed in Appendix B. These consist of (1) the lowest frequency at which the line has significant absorption, (2) the line intensity, (3) the pressure-broadening coefficient, (4) the lower state term value, (5) the molecule code number, and (6) $1/2$ the frequency range of significant absorption by the line. The program has a set of arrays in which the parameter values of the active lines are stored. The input file is sorted on the lowest contributing frequency values and NSPEC proceeds from the lowest observed frequency value, VL, to highest value, VU. The input file is processed in sequence and the active lines are sorted by NSPEC according to the highest frequency at which they have significant absorption. Because of this double sorting (i.e., sorted input file and sorted active list), when the transmittance at a new frequency position is to be calculated, the program needs to check only the first active line to see if any lines need to be removed from the active file. If the first line is still active at the new frequency, all the other lines are also still active. This eliminates the need to check every active line at every frequency position. If the first line is no longer active it is deactivated and the next line is checked. This continues until all lines which are not active at the new frequency position have been removed. The program then checks the next line in the input file. If it is not active at the new frequency, none of the lines below it in the file will be, and the program proceeds to calculate the transmittance. If the new line is active, it is inserted into the active list in the proper sequence and then the next input line is checked. This minimizes the number of checking operations required to maintain a correct list of active lines. Also, by not storing the parameters of inactive lines in core, the overall storage requirements of the program are reduced considerably.

In addition to the input parameters, the program stores the molecular masses (in amu) in the array FMAS. This value is needed to calculate the Doppler width. The active line parameters are stored in the arrays VO, SO, AMAS, ALL, EPP, MOLNM, and CENTW. Instead of sorting the elements of these seven arrays, an array of indices is kept, called IACTV, and these are kept in such a way that the order of the elements in IACTV determines the order in which the lines have to be checked for possible deactivation.

In order to calculate the convolved transmittance, τ_{con} , at observed frequency position, ν_i , the program must calculate the monochromatic transmittance, τ_{mon} , at frequency positions ν_1, \dots, ν_n (refer to Fig. 2). These are then multiplied by an instrument response (or slit) function value and summed to give τ_{con} . The storage of the τ_{mon} values in array T proved to be the most logically involved aspect of the calculation. The actual values are calculated quite simply using the Hui *et al.*²³ Voigt routine and summing absorption coefficients by layers and then by active lines in two nested DO-loops. The slit function value, called WT,

is evaluated, multiplied by the τ_{mon} values, and summed in another loop. The problem is how to store the τ_{mon} values so as to be able to retrieve them efficiently. This is all done by proper arrangement of the values in the array T.

First, the maximum number of τ_{mon} values is determined from NO and NM according to $\text{NTOT} = 2 \cdot 2^{\text{NM}} + 1$. The τ_{mon} values will then be stored in the first NTOT elements of T as if each position in T were a frequency position with a spacing between elements of $\text{DELVC} = \text{EXTNT} \cdot H / 2^{\text{NM}+1}$. This spacing fits the NTOT values into a total frequency range of $\text{EXTNT} \times H$, where H is one-half the full width at half height of the slit function.

To start off the calculation, the first element of the T-table is evaluated using NO to determine the number of points, as shown in Table A-3. Also listed are the number of new points (i.e., τ_{mon} values) used in subsequent iterations. The index n along the left-hand side of the table is used by the program to determine the maximum number of iterations. When the n value exceeds NM, the convolution stops iterating and takes the convergence failure error route.

For example, when NO = 1 and NM = 5, the first trapezoidal rule evaluation is made with five points. The corresponding τ_{mon} values are loaded into T. The next step involves a four-point midpoint rule evaluation. These two values are checked for convergence. If the convergence criterion is satisfied (AMTS.LE.EPA), the convolved transmittance value is loaded into the array TCI. If there is no convergence, an eight-point midpoint rule evaluation is done and the T- and M-table values calculated and compared. The procedure continues until convergence or until the 32-point midpoint rule value is calculated. After this value, the convergence failure route is taken. In this way, up to 65 τ_{mon} values would be calculated and loaded into array T in order of increasing frequency position. When moving to a new observed frequency position (next VI value), the new τ_{mon} values that need to be calculated are written on top of the old τ_{mon} values which are no longer needed. In this way space is conserved and the values of T can be efficiently retrieved.

As currently written, NSPEC generates its own observed frequency positions at which to calculate τ_{con} values. This can be easily changed to calculate τ_{con} values at specified nonuniformly spaced frequencies by passing the array of frequency positions to NSPEC and changing the scalar VI to an array V(I) of these frequency positions.

Table A3. The number of points in the first trapezoidal evaluation for different values of NO.

NO n						
	0	1	2	3	4	5
0	3					
1	2	5				
2	4	4	9			
3	8	8	8	17		
4	16	16	16	16	33	
5	32	32	32	32	32	65 . . .
.
.
.

```

//      TIME=4,REGION=512K
/*JGSPARM  LINES=4000,DISKID=3000
//NPL EXEC FORTXCG,PARM=(FORMAT,GOSTMT,
//      MAP,XREF,OPT(2)),TIME=4,REGION=512K
//FORT.SYSLIN DD DSN=TS0462.NSPEC.OBJ,DISP=(OLD,PASS),
//      SPACE=(TRK,(1,1))
//FORT.SYSLIN DD *
      DIMENSION UIN(300),PU(300),TU(300),U(50),PRES(50),TMP(50),
      * RMIXR(5,50),H(200),P(200),T(200),R(5)
      DIMENSION TCI(300)
      REAL*8 VL,VU
      COMMON H,P,T,UIN,PU,TU,IED,U,PRES,TMP,RMIXR
      READ(5,*) LEVELS,ALAT,Z,HOBS,NGE,LUNIT
      DO 100 I=1,LEVELS
      READ(10,*) H(I),T(I),P(I)
100 CONTINUE
      CALL SNIDER(LEVELS,ALAT,0,0,7,5.0,HOBS,82.0,1)
      READ(5,*) R(1),R(2),R(3),R(4),R(5)
      CALL PATHST(NGE,R,LEVTOP)
      READ(5,*) VL,VU,NVC,NM,NO,EPA,EXTNT,B,LINTOP,TTOP,NTST
      CALL NSPEC(VL,VU,NVC,NM,NO,EPA,EXTNT,B,LINTOP,LEVTOP,TTOP,
      * NTST,LUNIT,TCI)
      DO 500 I=1,NVC
      WRITE(12,110) TCI(I)
110 FORMAT(F8.5,1X,F11.5,1X,I3)
500 CONTINUE
      CALL ERROR(1,1)
      STOP
      END
      SUBROUTINE SNIDER(LEVELS,ALAT,NOPT,LSTOP,DD1,DD2,DD3,DD4,NLOPT)
      DIMENSION VARCOM(200)
      DIMENSION P(200)
      DIMENSION H(200),T(200),GRAD(200),GAMMA(200)
      DIMENSION Z(200)
      DIMENSION THETAS(200),DELTH(200)
      DIMENSION OMSTRA(200)
      DIMENSION AIRS(200)
      DIMENSION ESTR(200)
      DIMENSION RHO(200),ZRHO(200)
      DIMENSION XPTS(6),WGHT(6)
      REAL*8 TITLE(13)
      COMMON /SLANT/ VARCOM
      COMMON H,P,T
      EQUIVALENCE (VARCOM(1),G), (VARCOM(2),AIRWT), (VARCOM(3),
1 RSTAR), (VARCOM(4),RADIUS), (VARCOM(5),CONST1), (VARCOM(6)
2,XPTS(1)), (VARCOM(12),WGHT(1)), (VARCOM(18),FAKE)
      EQUIVALENCE (VARCOM(20),REFAM)
      REAL IP
      FCNA(Q000FL)=(1.0+Q000FL/2.0)*(1.0+2.0*Q000FL*(1.0+Q000FL/2.0)/3.0
1)/(1.0+Q000FL)**2
      FCNB(Q001FL)=2.0*Q001FL*(1.0+Q001FL/2.0)/3.0
      FCNC(Q002FL,Q003FL,Q004FL,Q005FL)=2.0*Q004FL*Q005FL*Q002FL/(1.0+Q000000210
103FL*Q005FL)
      FCNE(Q006FL,Q007FL)=Q006FL*(1.0-Q007FL)*(1.0-Q007FL*Q006FL/6.0)
      FHC(X)=GPHI * X/(RADIUS + X)
      FZC(Y)=RADIUS*Y/(GPHI - Y)
      NTATA2=5
      NERROR=6
      NTATA3=6
      RADSEC=.206264806E+06
      RADCON=.174532925E-01
      FAKE=-10000000.0

```

XPTS(1)=-.466234757E+00	00000320
XPTS(2)=-.330604693E+00	00000330
XPTS(3)=-.119309593E+00	00000340
XPTS(4)=-.119309593E+00	00000350
XPTS(5)=.330604693E+00	00000360
XPTS(6)=.466234757E+00	00000370
WGHT(1)=.056622491E-01	00000380
WGHT(2)=.180380786E+00	00000390
WGHT(3)=.233956967E+00	00000400
WGHT(4)=.233956967E+00	00000410
WGHT(5)=.180380786E+00	00000420
WGHT(6)=.056622491E-01	00000430
AVNMB= 6.02257 E26	00000440
IF (LEVELS.GT.190) CALL ERROR(1,0)	
LEVELS=MINO(LEVELS,190)	
1000 CONTINUE	00000450
C1000 READ (NTATA2,1021) (TITLE(I),I=1,13)	00000460
1021 FORMAT(13A6)	00000470
ALTORH=1.0	00000510
PHI = ALAT * RADCON	00000530
A = 6378160.0	00000540
B = 6356775.0	00000550
R = SQRT((A**4*(COS(PHI))**2 + B**4*(SIN(PHI))**2)/	00000560
1 (A**2*(COS(PHI))**2 + B**2*(SIN(PHI))**2))	00000570
X = COS(2.0 * PHI)	00000610
Y = COS(4.0 * PHI)	00000620
G = 980.6160 * (1.0 -(0.0026373 * X) + (0.0000059 *X**2))	00000630
G = G/100.0	00000640
PARTGZ = 3.085462 E-06 + 2.27 E-09 * X - 2.0 E-12 * Y	00000650
C RADIUS = 2.0 * G / PARTGZ	00000660
RADIUS =R	00000670
RSTAR=8314.39	00000680
AIRWT=28.966	00000690
CONST1=6*AIRWT/RSTAR	00000700
GEE = 9.80665	00000710
GPHI = RADIUS * G / GEE	00000720
DO 1 I=1,LEVELS	00000800
P(I)=P(I)*100.	00000810
H(I)=H(I)*1000.	00000820
1 CONTINUE	00000830
1051 CONTINUE	00000840
IF(P(1).EQ.0.) P(1)= 101325.0	00000850
DO 1090 I=2,LEVELS	00000860
CALL GETT(H(I-1),H(I),P(I-1),P(I),T(I-1),T(I))	00000870
1090 CONTINUE	00000880
IF(ALTORH) 1100,1150,1100	00000890
1100 CONTINUE	00000900
DO 1125 I=1,LEVELS	00000910
H(I) = FHC(H(I))	00000920
1125 CONTINUE	00000930
1150 CONTINUE	00000940
DO 1175 I=2,LEVELS	00000950
GRAD(I-1)=(T(I)-T(I-1))/(H(I)-H(I-1))	00000960
GAMMA(I-1)=(CONST1)/(GRAD(I-1)+CONST1)	00000970
DELTH (I-1)= H(I) -H(I-1)	00000980
1175 CONTINUE	00000990
GAMMA(LEVELS) = 1.	00001000
GRAD(LEVELS) = 0.	00001010
DELTH(LEVELS) = 0.0	00001020
SUMRHU = 0.0	00001030
DO 1190 I = 1,LEVELS	00001040
ZKHO(I) = AVNMB * P(I) /(RSTAR * T(I))	00001050

	SUMKHO = SUMRHO + ZRHO(I) * DELTH (I)	00001060
1190	CONTINUE	00001070
	RHO(1) = ZRHO(1)	00001080
	OMSTRU = 1.0 -(RHO(1) / 2.5475521 E25)	00001090
	DO 1200 I=2,LEVELS	00001100
	CALL OM (H(I),H(I-1),H(I-1),T(I-1),GAMMA(I-1),OMEGA, DUMMY)	00001110
	NLC = I-1	00001120
	OMSTRA(NLC)=OMEGA	00001130
	RHO(I)=RHO(I-1)*(1.0-OMEGA)	00001140
	CALL OPT1(H(I-1),H(I),T(I-1),GAMMA(I-1),RHO(I-1),OMEGA,AIRS(I-1)	00001150
	1)	00001160
1200	CONTINUE	00001170
	AIRS(LEVELS)=0.0	00001180
	DO 1225 I=2,LEVELS	00001190
	IND=LEVELS+1-I	00001200
	AIRS(IND)=AIRS(IND)+AIRS(IND+1)	00001210
1225	CONTINUE	00001220
	STARD = AIRS(1)	00001230
C	REFAM = AIRS(1)	00001240
	REFAM = 2.15335 E29	00001250
1243	FORMAT(1H1)	00001420
	LINC=1	00001430
	ALTORH=1.0	00001470
	CALL POUT(-1.0,1.0,1.0)	00001475
1250	CONTINUE	
	DD3=DD3*1000.0	00001490
	DD4 = DD4*1000.0	00001500
	NLOP = 0	00001510
	JMP=LSTOP+1	00001520
	NTF=0	00001530
	LINC=-1	00001540
	GO TO (1257,1257,1257,1256,1000), JMP	
1256	GO TO 1400	00001560
1257	DO 4150 IN=1,50	00001570
	NTF=0	
	NLOP = NLOP + 1	00001610
	IF (NLOP.GT.NLOPT) GO TO 1400	00001620
1297	CONTINUE	00001630
	ZO=DD1	00001640
	ZOS=ZC	00001650
	OHGHT=DD3	00001660
	HGHT=DD4	00001670
1258	WAVEL=DD2	00001680
	ZO=ZOS	00001690
1270	IF(ALTORH) 1280,1290,1280	00001700
1280	OHGHT=FHC(OHGHT)	00001710
	HGHT =FHC(HGHT)	00001720
1290	CONTINUE	00001730
	ZCS=ZO	00001740
	ZT=ZOS	00001750
1295	CONTINUE	00001760
	NTF=NTF+1	
	IF (NTF-10) 1296,1296,4700	00001770
1296	CONTINUE	00001780
	SECT2=C.	00001790
	SECT3 = 0.0	00001800
	SECT4 = 0.0	00001810
	RSAVE=0.	00001820
	OSAVE=0.	00001830
	PSAVE= 0.0	00001840
	TSAVE= 0.0	00001850
	HDIFF = 0.0	00001860

HTAN = 0.0	00001870
TP = 273.15	00001880
TG=TP	00001890
ZG=Z0*RA9CSN	00001900
UTEMP=1.0/WAVEL**2	00001910
E1 = 0.0	00001920
E1=.00064328+.0294981/(146.0-UTEMP)+.0002554/(41.0-UTEMP)	00001930
DO 1360 IHT=2,LEVELS	00001940
IF(H(IHT)-DHGHT) 1300,1325,1325	00001950
1300 CONTINUE	00001960
CALL ERROR(2,0)	
RETURN	
1325 IHT=IHT-1	00001990
CALL GETT (H(IHT), DHGHT, P(IHT), POB, T(IHT), T(IHT))	00002000
RHOP = AVINMB * POB/(RSTAR*T(IHT))	00002010
RHOMIN = RHOP	00002020
TP = T(IHT)	00002030
DO 1335 IND= 2,LEVELS	00002040
JHT=IND	00002050
IF(H(JHT)-HGHT) 1335,1340,1340	00002060
1335 CONTINUE	00002070
CALL ERROR(3,0)	
1337 FORMAT(20H UPPER HEIGHT RESET)	00002090
1330 JHT=IND	00002100
1340 CONTINUE	00002110
ESTR (1) = FCNE (E1 , OMSTRO)	00002120
DO 1350 I=2,LEVELS	00002130
ESTR(I)=FCNE(ESTR(I-1),OMSTRA(I-1))	00002140
1350 CONTINUE	00002150
JNS=1	00002160
HMINA=DHGHT	00002170
IF (ZG.LE.90.) IF (HGHT-DHGHT+.05) 4500,4600,1373	00002180
CALL UM(DHGHT,H(IHT),H(IHT),T(IHT),GAMMA(IHT),OME,XXX)	00002190
EO=FCNE(ESTR(IHT),OME)	00002200
ZCRIT = ASIN ((1.0 + ESTR (1)) * (1.0 - DHGHT / RADIUS) / (1.0	00002210
1 + EO))	00002220
ZCRIT=3.141592653-ZCRIT	00002230
IF (ZG.GT.ZCRIT+.00001) IF (DHGHT-HGHT+.05) 4500,4600,1357	00002240
FVAL = SIN(ZG)*(1.+EO)/(RADIUS-DHGHT)	00002250
F1=(1.+ESTR(1))/RADIUS - FVAL	00002260
DO 1351 I=2,LEVELS	00002270
K=I-1	00002280
F2=(1.+ESTR(I))/(RADIUS-H(I))-FVAL	00002290
IF(F2*F1) 1352,1352,1351	00002300
1351 F1=F2	00002310
GO TO 4500	00002320
1352 H1=H(K)	00002330
H2=H(K+1)	00002340
H3=H1-(H2-H1)*F1/(F2-F1)	00002350
1353 CALL UM(H3,H(K),H(K),T(K),GAMMA(K),W,XXX)	00002360
F3=(1.+FCNE(ESTR(K),W))/(RADIUS-H3)-FVAL	00002370
H4=H3-F3*((H3-H2)/(F3-F2)+(H3-H1)/(F3-F1)-(H2-H1)/(F2-F1))	00002380
IF (ABS(HM-H3).LE.1.) GO TO 1354	00002390
H1=H2	00002400
H2=H3	00002410
H3=HM	00002420
F1=F2	00002430
F2=F3	00002440
GO TO 1353	00002450
1354 IF (HM.GT.HGHT+.05) GO TO 4500	00002460
HMINA=HM	00002470
ZGSAVE=ZG	00002480

HOSAVE=JHGHT	00002490
HSSAVE=HGHT	00002500
ZO=1.570796326	00002510
OHGHT=HM	00002520
HGHT=HOSAVE	00002530
TG=T (K)	00002540
JSAY=JHT	00002550
JHT=IHT+1	00002560
IHT=K	00002570
INS=2	00002580
GO TO 1374	00002590
1355 RSAVE=REFRS	00002600
OSAVE=SECT2	00002610
PSAVE = SECT3	00002620
TSAVE = SECT4	00002630
HGHT=HSSAVE	00002640
JHT=JSAY	00002650
INS=3	00002660
GO TO 1374	00002670
1356 IF(HSSAVE.LT.HOSAVE) JNS=2	00002680
OHGHT=HOSAVE	00002690
GO TO 3950	00002700
1357 CALL OM(HGHT,H(JHT),H(JHT),T(JHT),GAMMA(JHT),W,XXX)	00002710
ZSAVE=ASIN((1.+EO)/(1.+FCNE(ESTR(JHT),W))*(RADIUS-HGHT)/(RADIUS-	00002720
1OHGHT))	00002730
IHT=JHT	00002740
ZZ=ZO	00002750
ZO=ZSAVE	00002760
HOSAVE=OHGHT	00002770
HSSAVE=HGHT	00002780
OHGHT=HSSAVE	00002790
HGHT=HOSAVE	00002800
ZO=ZZ	00002810
INS=4	00002820
GO TO 1374	00002830
1358 JNS=1	00002840
OHGHT=HOSAVE	00002850
HGHT=HSSAVE	00002860
GO TO 3950	00002870
1373 INS=1	00002880
1374 CONTINUE	00002890
CALL OM(OHGHT,H(IHT),H(IHT),T(IHT),GAMMA(IHT),OME,DUMMY)	00002900
CALL OM(H(IHT+1),OHGHT,H(IHT),T(IHT),GAMMA(IHT),OMO,TOO)	00002910
EO=FCNE(ESTR(IHT),OME)	00002920
VARCOM(19)=RHO(IHT)*(1.-OME)	00002930
IF(JHT.EQ.IHT+1) GO TO 1380	00002940
US=FCNU(FCNA(EO),FCNB(EO),EC,OMG)	00002950
CALL ZCOMP(ZO,Z(IHT+1),OHGHT,H(IHT+1),US,DELZ,THETAS(IHT+1)	00002960
1)	00002970
CALL QUAD(THETAS(IHT+1),ZO,OHGHT,TOO,P(IHT+1),GAMMA(IHT),EO,SECT1,	00002980
1SECT2,SECT3,SECT4)	00002990
CALL POUT(SECT2,SECT3,SECT4)	00002994
REFR=(DELZ+SECT1)	00003000
REFRS=REFR*RADSEC	00003010
2010 DELRS=REFRS	00003020
2060 INDU=JHT-2	00003030
IHT1=IHT+1	00003040
IF(INDU.LT.IHT1) GO TO 1376	00003050
1360 CONTINUE	00003060
DO 1375 I=IHT1,INDU	00003070
U=FCNU(FCNA(ESTR(I)),FCNB(ESTR(I)),ESTR(I),OMSTRA(I))	00003080
CALL ZCOMP(Z(I),Z(I+1),H(I),H(I+1),U,DELZ,THETAS(I+1))	00003090

DELZT=DELZT+DELZ	00003100
VARCOM(19)=RHC(I)	00003110
CALL QUAD(THETAS(I+1),Z(I),H(I),T(I),P(I),GAMMA(I),ESTR(I),ADD1,	00003120
1ADD2,ADD3,ADD4)	00003130
CALL POUT(ADD2,ADD3,ADD4)	00003135
SECT2=SECT2+ADD2	00003140
SECT3 = SECT3 + ADD3	00003150
SECT4 = SECT4 + ADD4	00003160
DELR = (DELZ+ADD1)	00003170
REFR = DELR+REFR	00003180
REFRS=REFR*RADSEC	00003190
DELD=DELR*RADSEC	00003200
1375 CONTINUE	00003210
1376 CONTINUE	00003220
RULAST=RHO(JHT-1)	00003230
ZLAST=Z(JHT-1)	00003240
ELAST=ESTR(JHT-1)	00003250
PLAST = P(JHT-1)	00003260
TLAST=T(JHT-1)	00003270
GLAST=GAMMA(JHT-1)	00003280
HLAST=H(JHT-1)	00003290
1377 CONTINUE	00003300
CALL UM(HGHT,HLAST,H(JHT-1),TLAST,GLAST,OLAST,XXX)	00003310
U=FCNU(FCNA(ELAST),FCNB(ELAST),ELAST,OLAST)	00003320
CALL ZCUMP(ZLAST,ZFIN,HLAST,HGHT,L,DELZ,THFIN)	00003330
VARCOM(19)=ROLAST	00003340
CALL QUAD(THFIN,ZLAST,HLAST,TLAST,PLAST,GLAST,ELAST,ADD1,ADD2,ADD3	00003350
1,ADD4)	00003360
CALL POUT(ADD2,ADD3,ADD4)	00003365
SECT3 = SECT3 + ADD3	00003370
SECT4 = SECT4 + ADD4	00003380
DELR=DELZ+ADD1	00003390
REFR=DELR+REFR	00003400
REFRS=REFR*RADSEC	00003410
SECT2=SECT2+ADD2	00003420
DELD=DELR*RADSEC	00003430
IF (INS.EQ.2) GO TO 1355	00003440
KJHT=JHT-1	00003450
GO TO (3950,1355,1356,1358),INS	00003460
1380 ROLAST=VARCOM(19)	00003470
ZLAST=Z0	00003480
ELAST=E0	00003490
HLAST=OHGHT	00003500
TLAST=T(JHT-1)	00003510
PLAST = P(JHT-1)	00003520
GLAST=GAMMA(JHT-1)	00003530
REFR=U.	00003540
GO TO 1377	00003550
3950 CONTINUE	00003560
SECT3 = SECT3 + PSAVE	00003570
SECT4 = SECT4 + TSAVE	00003580
REFRS=REFRS+RSAVE	00003590
SECT2=SECT2+OSAVE	00003600
DERF=REFRS/3600.	00003610
ZEND=ZOS+DERF	00003620
PEFF = SECT3/SECT2	00003630
TEFF = SECT4/SECT2	00003640
IF(JMP.EQ.2) GO TO 4100	00003650
3980 CONTINUE	00003660
IF (LINC) 3990,3999,3999	00003670
3990 CONTINUE	00003680
C3990 WRITE(NTATA3,3991) TITLE	00003690

```

3991 FORMAT(1H1,5X25HREFRACTION AIRMASS TABLES,5X13A6,/,
340X38HALL HEIGHTS ARE IN GEOMETRIC METERS /,40X,'ALL TEMPERATUR00003710
3ES ARE IN DEGREES KELVIN'/,40X,'ALL PRESSURES ARE IN N/SQ M '/ 00003720
440X40HTHE APPARENT AND ASTRONOMICAL ANGLES ARE/ 00003730
540X34HIN DECIMAL DEGREES FROM THE ZENITH/) 00003740
C WRITE (6,3993) WAVELENGTH
3993 FORMAT (40X 'THE WAVELENGTH FOR THIS TABLE IS ',F5.2,' MICROMETER00003760
IS.'//) 00003770
C WRITE(6,3992)
3992 FORMAT(11X5HLOWER,5X5HUPPER,5X4HMIN.,7X7HCHAPMAN,5X7HOPTICAL)00003790
C WRITE(6,3995)
3995 FORMAT(1X5HAPP.,2,4X5HHEIGHT,4X6HHEIGHT,4X6HHEIGHT,5X8HAIR MASS,4X00003810
18HAIR MASS,4X5HHDIFF,3X10HREFRACTION,4X6HAST.Z,6X6HP(EFF),4X6H00003820
IT(EFF),6X6HP(TAN) ) 00003830
C WRITE(6,3996) 00003840
3996 FORMAT(5X3H(1),7X3H(2),7X3H(3),7X3H(4),8X3H(5),8X3H(6),10X3H(7), 00003850
16X3H(8),9X3H(9),9X4H(10),6X4H(11),8X4H(12),/,1X ) 00003860
LINC=42 00003870
3999 LINC=LINC-1 00003880
ZFIN = ZEND * RADCON 00003890
OHGHT = FZC (OHGHT ) 00003900
HGMT = FZC (HGMT ) 00003910
HMINA = FZC (HMINA) 00003920
SCALHP = RSTAR * TP /AIRWT / G 00003930
XP = ( RADIUS + OHGHT ) / SCALHP 00003940
WHY = SQRT ( 0.5 * XP ) * ABS (COS(ZFIN)) 00003950
FERF = EXP((WHY)**2.0) * ( 1.0 - ERF (WHY)) 00003960
4040 CONTINUE 00004210
4150 CONTINUE 00004270
LSTOP = 3 00004275
GO TO (1250,4100,1250,1256,1000),JMP 00004280
4160 CONTINUE 00004290
IF (ABS(ZT-ZEND).LT.0.0001) GOTO 4200
ZOS=ZT *ERF
ZO=ZOS 00004310
GO TO 1295 00004320
4200 JMP=1 00004330
GO TO 3980 00004340
4500 CALL ERROR(4,0) 00004350
4510 FORMAT(1XF14.5,6CX20H *** NO SOLUTION ***) 00004370
LINC=LINC-1 00004380
RETURN
4600 REFRS=C. 00004400
SECT2=C. 00004410
SECT3=C. 00004420
SECT4=C. 00004430
GO TO 3950 00004440
4700 IF (ABS(ZT-ZEND).LT..001) GO TO 4200 00004450
LINC=LINC-2 00004460
CALL ERROR(5,0)
4705 FORMAT(14,37H***NO GCOL SOLUTION FOR LINE ABOVE***) 00004500
4003 FORMAT(1H ' UNREFRACTED RAY STRIKES DISC ') 00004520
RETURN
1400 CONTINUE 00004540
RETURN
END 00004560
SUBROUTINE UM(H,HC,HV,TN,GAMMA,OMEGA,TO) 00004610
COMMON /SLANT/ G,AIRWT,RSTAR,RADIUS,CONST1 00004620
GM=ABS(GAMMA) 00004630
IF(GM.LT.0.0000001)GO TO 801 00004640
ONEG=1.0-GAMMA 00004650
ONG=ONEG 00004660

```


	IF(RADIUS+HN) 500,500,600	00004670
500	CONTINUE	00004680
	X=CONST1*H*(RADIUS-HC)/TN	00004690
	GO TO 700	00004700
600	CONTINUE	00004710
	A=CONST1*(H-HC)	00004720
	TO=TN+CONST1*(HC-HN)*(ONG)/GAMMA	00004730
	X=A/TO	00004740
700	CONTINUE	00004750
	Y=-X/GAMMA	00004760
	IF(ONEG.EQ.0.) GO TO 800	00004770
	IF(1.0-ONEG*Y) 803,803,400	00004780
400	IF(1.0-(1.0-ONEG*Y)) 800,800,300	00004790
300	OMEGA=1.-(1.-ONEG*Y)**(-1./ONEG)	00004800
	RETURN	00004810
500	CONTINUE	00004820
	IF(Y.LT.(-30.0))Y=0.0	00004830
1	FORMAT(1H,5E20.8)	00004840
	IF(ABS(Y).GT.25.0) GO TO 10	00004850
	OMEGA=1.0-EXP(Y)	00004860
10	CONTINUE	00004870
	RETURN	00004880
801	CALL ERKOR(6,C)	
802	FORMAT(1X,8H GAMMA=0)	00004900
803	CALL ERROR(7,0)	
804	FORMAT(1,30E20.8)	00004920
	RETURN	00004950
	END	00004960
	SUBROUTINE UPT1(HC,H,TO,GAMMA,RHOC,OMEGA,AIRM)	00004970
	COMMON /SLANT/ G,AIRWT,RSTAR,RADIUS,CONST1	00004980
	RAD=RADIUS-HC	00004990
	XK=CONST1*RAD/(TO*GAMMA)	00005000
	SMALLH=(H-HC)/(RADIUS-HC)	00005010
	ONEH=1.0-SMALLH	00005020
	ONEG=GAMMA-1.0	00005030
	XK2=(1.0-ONEG*SMALLH*XK)/ONEH	00005040
	SUMU=0.0	00005050
	SUMV=0.0	00005060
	XN=0.0	00005070
	DENOM=1.0	00005080
	TERMU=1.0	00005090
	TERMV=1.0	00005100
	TEST=.0000001/(XK*GAMMA)	00005110
	KOUNT=0	00005120
1000	CONTINUE	00005130
	KOUNT=KOUNT+1	00005140
	XN=XN+1.0	00005150
	DENOM=DENOM+ONEG	00005160
	FACT=XN/(XK*DENOM)	00005170
	TERMU=TERMU*FACT	00005180
	TERMV=TERMV*FACT*XK2	00005190
	SUMU=SUMU+TERMU	00005200
	SUMV=SUMV+TERMV	00005210
	IF (KOUNT-31) 1040,1040,1080	00005220
1040	IF(ABS(TEST)-ABS(TERMV)) 1000,1000,1050	00005230
1050	IF(ABS(TEST)-ABS(TERMU)) 1000,1000,1075	00005240
1075	IF (KOUNT-30) 1100,1100,1080	00005250
1080	WRITE(6,1085)	00005260
1085	FORMAT(17H0 50000 IN CPT1)	00005270
1100	AIRM=(RADIUS**2/RAD)*RHOC*(SUMU-(1.0-OMEGA)*SUMV/ONEH)	00005280
	RETURN	00005290
	END	00005300

FUNCTION ASINX(X)	00005310
Z=X**2	00005320
ASINX=X*(1.+Z/6.+0.075*Z**2)	00005330
RETURN	00005340
END	00005350
SUBROUTINE ZCOMP(ZC,ZS,H0,HS,US,DELZ,THETA)	00005360
COMMON /SLANT/ G,AIRWT,RSTAR,RADIUS,CONST1	00005370
SMALLH=(HS-H0)/(RADIUS-H0)	00005380
ONEH=1.0-SMALLH	00005390
TWOH=SMALLH*(2.0-SMALLH)	00005400
C=COS(ZC)	00005410
S=SIN(ZC)	00005420
CONE=C*ONEH	00005430
CPLUS=CONE**2+TWOH	00005440
DELZ=S*(US-TWOH)	00005450
DEL3=SQRT(1.0-US)*(CONE+SQRT(CPLUS-US))	00005460
DEL=S*TWOH/(CONE+SQRT(CPLUS))	00005470
DELZ=ASINX(DEL2/DEL3)	00005480
ZS=ZC+DELZ	00005490
THETA=ASINX(DEL)	00005500
RETURN	00005510
END	00005520
SUBROUTINE QUAD(THETA,ZC,H0,T,P,GAMMA,EO,SUM,VALM,PBAR,TBAR)	00005530
DIMENSION VALUEA(6)	00005540
DIMENSION VARCOM(50)	00005550
DIMENSION HINT(6)	00005560
DIMENSION XPTS(6),THTPTS(6),WGHT(6),VALUES(6)	00005570
COMMON /SLANT/ VARCOM	00005580
EQUIVALENCE (VARCOM(1),G), (VARCOM(2),AIRWT), (VARCOM(3),	00005590
1 RSTAR), (VARCOM(4),RADIUS), (VARCOM(5),CONST1), (VARCOM(6)	00005600
2,XPTS(1)), (VARCOM(12),WGHT(1)), (VARCOM(18),FAKE)	
EQUIVALENCE (VARCOM(20),REFAM)	00005620
EQUIVALENCE (VARCOM(19),RHO)	00005630
FCNA(Q000FL)=(1.0+Q000FL/2.0)*(1.0+2.0*Q000FL*(1.0+Q000FL/2.0)/3.0	00005650
1)/(1.0+Q000FL)**2	00005660
FCNB(Q001FL)=2.0*Q001FL*(1.0+Q001FL/2.0)/3.0	00005670
FCNJ(Q002FL,Q003FL,Q004FL,Q005FL)=2.0*Q004FL*Q005FL*Q002FL/(1.0+Q000005680	
103FL*Q005FL)	00005690
FCNH(Q008FL,Q009FL)=2.0*SIN(Q008FL/2.0)**2+COTAN(Q009FL)*SIN(Q008F00005700	
2L)	00005710
SMALLR=RADIUS+H0+H0**2/(RADIUS-H0)	00005720
VALC=RHO*SMALLR*SIN(ZC)*THETA/REFAM	00005730
A=FCNA(EO)	00005740
B=FCNB(EO)	00005750
DO 1000 I=1,6	00005760
THTPTS(I)=THETA*(.5+XPTS(I))	00005770
HINT(I)=FCNH(THTPTS(I),ZC)	00005780
1000 CONTINUE	00005790
DO 2000 I=1,6	00005800
CALL GM(HINT(I),H0,FAKE,T,GAMMA,OMEGA,DUMMY)	00005810
U=FCNJ(A,B,EO,OMEGA)	00005820
ARG1=1.0-U/COS(ZC-THTPTS(I))**2	00005830
VALUES(I)=1./SQRT(ARG1)	00005840
VALUEA(I)=VALUES(I)*(1.-OMEGA)*SQRT(1.-U)/SIN(ZC-THTPTS(I))**2	00005850
2000 CONTINUE	00005860
SUM=0.0	00005870
VALM=0.	00005880
DO 3000 I=1,6	00005890
SUM=VALUES(I)*WGHT(I)+SUM	00005900
VALM=VALM+VALUEA(I)*WGHT(I)	00005910
3000 CONTINUE	00005920
SUM=SUM*THETA	00005930

VALM=VALC*VALM	00005940
PEAK = VALM*P	00005950
TBAK = VALM*T	00005960
RETURN	00005970
END	00005980
SUBROUTINE GETT(H1,H2,P1,P2,T1,T2)	00005990
COMMON /SLANT/ G,AIRWT,RSTAR,RADILS,CONST1	00006000
IF(T2.GT.0.) GO TO 1700	00006010
K=C	00006020
X=P2/P1	00006030
XL=ALOG(X)	00006040
A1=CONST1*(H2-H1)/T1	00006050
CRIT=EXP(-A1)	00006060
A1=1./A1	00006070
IF(ABS(X-CRIT).GT..000001) GO TO 1000	00006080
T2=T1	00006090
RETURN	00006100
1000 XC=A1*XL+ALOG(A1)	00006110
ACRIT=-1./XL	00006120
AZ=.000001	00006130
IF(A1.LT.ACRIT) A2=A2+ACRIT	00006140
1100 F=A2*XL+ALOG(A2)-XC	00006150
FP=XL+1./A2	00006160
A3=A2-F/FP	00006170
IF(K.LT.3) GO TO 1200	00006180
IF(ABS(A3-A2).LT..0000001) GO TO 1300	00006190
1200 A2=A3	00006200
K=K+1	00006210
GO TO 1100	00006220
1300 T2=T1*A2/A1	00006230
RETURN	00006240
1700 IF(T1.EQ.T2) GO TO 1800	00006250
P2=P1*(T2/T1)**((CONST1*(H2-H1))/(T1-T2))	00006260
RETURN	00006270
1800 P2=P1*EXP(CONST1*(H1-H2)/T1)	00006280
RETURN	00006290
END	00006300
SUBROUTINE POUT(A1,A2,A3)	00006310
DIMENSION UED(300),TED(300),PED(300),H(200),P(200),T(200)	
COMMON H,P,T,UED,PED,TED,IED	
IF (A1.EQ.-1.0) GO TO 100	
IED=IED+1	
UED(IED)=A1*0.215335E26	
PED(IED)=A2*0.215335E26	
TED(IED)=A3*0.215335E26	
RETURN	
100 IED=0	
RETURN	
END	
SUBROUTINE FATHST(NGE,RN,LEVTOP)	
DIMENSION UIN(300),PU(300),TU(300),U(50),PRES(50),TMP(50),	
* RMIXR(5,50),HT(200),PP(200),TP(200),RN(5)	
COMMON HT,PP,TP,UIN,PU,TU,IED,U,PRES,TMP,RMIXR	
FTOT=0.0	
DO 50 I=1,IED	
50 FTOT=FTOT+UIN(I)	
DO 100 I=2,IED	
IF (ABS(UIN(I)-UIN(1)).LE.0.001) GOTO 120	
100 CONTINUE	
NFOLD=0	
GO TO 220	
120 NFOLD=I-1	

```

      DO 200 J=1,NFOLD
      K=NFOLD+J
      UIN(K)=UIN(J)+UIN(K)
      PU(K)=PU(J)+PU(K)
      TU(K)=TU(J)+TU(K)
200  CONTINUE
220  J1=NFOLD+1
      K=0
      IF (FTOT.LE.0.001) CALL ERROR(9,0)
      SUMU=0.0
      SUMP=0.0
      SUMTU=0.0
      DO 400 J=J1,IED
      SUMU=SUMU+UIN(J)
      SUMP=SUMP+PU(J)
      SUMTU=SUMTU+TU(J)
      IF (SUMU.GT.FTOT/NGE) GO TO 390
      GO TO 400
390  K=K+1
      U(K)=SUMU
      PRES(K)=SUMP/SUMU
      TMP(K)=SUMTU/SUMU
      SUMU=0.0
      SUMP=0.0
      SUMTU=0.0
      IF (J.EQ.IED) GO TO 420
400  CONTINUE
      K=K+1
      U(K)=SUMU
      PRES(K)=SUMP/SUMU
      TMP(K)=SUMTU/SUMU
420  CONTINUE
      DO 600 J=1,K
      DO 500 IJ=1,5
      RMIXR(IJ,J)=RMIX(IJ,PRES(J),RN)
500  CONTINUE
600  CONTINUE
      LEVTOP=K
      RETURN
      END
      FUNCTION RMIX(I,P,RN)
      DIMENSION RN(5)
      RMIX=RN(I)
      RETURN
      END
      SUBROUTINE NSPEC(VL,VU,NVO,NM,NO,EPA,EXTNT,H,LINTOP,NLEVL,
*TTOP,NTST,IUNIT,TCI)
      COMPLEX*16 A0/(1.22697931777104326D02,0.0001)/,A1/
      +(2.14382388694706425D02,0.0001)/,A2/(1.81928533092181549D02,
      +0.0001)/,A3/(9.3155580458138441D01,0.0001)/,A4/
      +(3.01600142196210589D01,0.0001)/,A5/(5.912626209773153D0,0.0001)/
      +,A6/(0.564189583582815D0,0.0001)/,B0/(1.2269793177387535D02,
      +0.0001)/,B1/(3.52730625110963558D02,0.0001)/,B2/
      +(4.57534478785897737D02,0.0001)/,B3/(3.48703917719495792D02,
      +0.0001)/,B4/(1.70354001821091472D02,0.0001)/,B5/
      +(5.3992900912940267D01,0.0001)/,B6/(1.0479857114260399D01,
      +0.0001)/,Z1,F,DC,PLX
      DIMENSION HX(200),PX(200),TX(200),UINX(300),PUX(300),TUX(300)
      REAL*8 ZVUIGT,X,Y,ABSK,V0,V1,VK,VIK,VL,VU,V8H,VONXT,VOL,VUP,D2ABS
      DIMENSION VG(200),SG(200),ALL(200),EPP(200),TCI(300),
      2 MOLNM(200),NH(7),NSTA(7),T(260),AMK(8),PRES(50),TMP(50),
      3 U(50),RMIXR(5,50),IACTV(200),AMAS(200),CENTW(200)

```

REAL FMAS(5)/18.0,44.0,48.0,40.0,28.0/	00000180
INTEGER VART(5)/3,2,3,2,2/	00000190
COMMON HX,PA,TX,UIX,PUX,TUX,IEDX,U,PRES,TMP,RMIXR	00000200
CALL UNDRFL	00000210
ASSIGN 137 TO ISWT	00000220
IF(VU.LE.VL) GOTO 1350	
NLINES=0	00000230
ITAIL=1	00000240
DO 20 JL=1,200	00000250
20 IACTV(JL)=JL	00000260
PC=101330.	00000270
T0=273.	00000280
CONST2=ALOG(2.)	00000290
ALN2=SQRT(CONST2)	00000300
PI=3.141592654	00000310
CONST1=ALN2/SQRT(PI)	00000320
IF (NM.GT.7) CALL ERROR(10,0)	
NM=MIN0(NM,7)	
WID=EXTNT*H/2.	00000340
NTOT=2*2**NM + 1	00000350
READ(1UNIT,9010,END=1340) VCNXT,SCNXT,ALLNXT,EPPNXT,MOLNXT,CWNXT	00000360
9010 FORMAT(F9.3,E10.3,F6.3,F9.3,I2,F6.3)	00000370
VONXT=VCNXT+CWNXT	00000380
DELVC=EXTNT*H/FLOAT(2**((NM+1)))	00000390
110 I=1	00000400
VI=VL	00000410
120 NBH=1	00000420
VBH=VI-DELVC*FLOAT(NTOT-1)/FLOAT(2)	00000430
NH(1)=-2**((NM-NO))	00000440
NSTW(1)=-2**((NM-NO))	00000450
MTOP=NM-NO+1	00000460
DO 125 M=2,MTOP	00000470
NH(M)=-2**((NM+1-NO-M))	00000480
NSTW(M)=-2**((NM+2-NO-M))	00000490
125 CONTINUE	00000500
EPA=EPA/FLOAT(NSTW(1))/DELVC	00000510
130 NWL=1	00000520
NST=NSTW(NWL)	00000530
K=NH(1)+NST	00000540
NOUT=0	00000550
IF(NLINES.LE.0) GOTO 132	00000560
131 IF((V0(IACTV(ITAIL))+CENTW(IACTV(ITAIL)).GT.VI-WID) GOTO 132	00000570
ITAIL=MOD(ITAIL,LINTOP)+1	00000580
NOUT=NOUT+1	00000590
IF(NOUT.LT.NLINES) GOTO 131	00000600
132 NLINES=MAX0(0,NLINES-NOUT)	00000610
133 IF(VONXT-CWNXT.GT.VI+WID) GOTO 138	00000620
IF(VCNXT+CWNXT.LT.VI-WID) GOTO 136	00000630
ILOAD=IACTV(100(ITAIL+NLINES-1,LINTOP)+1)	00000640
V0(ILOAD)=VCNXT	00000650
SC(ILOAD)=SCNXT*CONST1	00000660
AMAS(ILOAD)=VCNXT*3.58133E-07/SQRT(FMAS(MOLNXT))	00000670
ALL(ILOAD)=ALLNXT*ALN2/PC*SQRT(T0)/AMAS(ILOAD)	00000680
EPP(ILOAD)=-EPPNXT/0.6946/T0	00000690
MOLNXT(ILOAD)=MOLNXT	00000700
CENTW(ILOAD)=CWNXT	00000710
V0P=VCNXT+CWNXT	00000720
J=NLINES-1	00000730
NLINES=NLINES+1	00000740
IF(NLINES.GT.LINTOP) GOTO 1340	00000750
IF(NLINES.EQ.1) GOTO 136	00000760
134 K1=MOD(ITAIL+J-1,LINTOP)+1	00000770

INXT=IACTV(K1)	00000780
IF(VUP.GE.VU(INXT)+CENTW(INXT)) GOTO 136	00000790
K2=MOD(1TAIL+J,LINTUP)+1	00000800
IACTV(K2)=INXT	00000810
IACTV(K1)=ILCAD	00000820
IF(J.EQ.0) GOTO 136	00000830
J=J-1	00000840
GO TO 134	00000850
136 CONTINUE	00000860
GO TO ISNT,(137,138)	00000870
137 READ(IUNIT,9010,END=133C) VCNXT,SCNXT,ALLNXT,EPPNXT,MOLNXT,CWNXT	00000880
VONXT=VCNXT+CWNXT	00000890
GO TO 133	00000900
138 CONTINUE	00000910
IF(NLINES.LE.0) GOTO 1320	00000920
140 VK=VBH+DELVC*FLOAT(K)	00000930
IF(K.GE.NTOT) GOTO 410	00000940
ABSK=0.	00000950
DO 200 L1=1,NLINES	00000960
L=IACTV(MOD(1TAIL+L1-2,LINTCP)+1)	00000970
MOLNML=MOLNM(L)	00000980
SOL=SO(L)	00000990
VOL=(VK-VG(L))*ALN2	00001000
ALLL=ALL(L)	00001010
AMASL=AMAS(L)	00001020
EPPL=EPP(L)	00001030
NPARTL=NPART(MOLNML)	00001040
DO 300 IAT=1,NLEVL5	00001050
TEMP=TMP(IAT)	00001060
RT=T0/TEMP	00001070
ALD=AMASL*SQRT(TEMP)	00001080
BOLT=SQRT(RT**NPARTL)*EXP(EPPL*(RT-1.))	00001090
AKO=U(IAT)*SOL*BOLT/ALD*RMIXR(MOLNML,IAT)	00001100
Y=ALLL*PRES(IAT)/TEMP	00001110
X=VOL/ALD	00001120
ZH=UCHPLX(Y,-X)	00001130
F=(((((A0*ZH+A5)*ZH+A4)*ZH+A3)*ZH+A2)*ZH+A1)*ZH+A0)	00001140
Z/(((((Zn+B6)*ZH+B5)*ZH+B4)*ZH+B3)*ZH+B2)*ZH+B1)*ZH+B0)	00001150
ZVOIGT=F	00001160
DZABS=AKO*ZVOIGT	00001170
ABSK=ABSK+DZABS	00001180
300 CONTINUE	00001190
IF(ABSK.GT.TTOP) GOTO 210	00001200
200 CONTINUE	00001210
210 NK=MOD(NBH+K-1,NTOT)+1	00001220
T(NK)=DEXP(-ABSK)	00001230
C IF(NTST.EQ.2) WRITE(14,9014) T(NK),VK	00001240
9014 FORMAT(' ',F8.5,1X,F11.5)	00001250
K=K+NST	00001260
400 GO TO 140	00001270
410 NHC=K-NST	00001280
CONVT=C.	00001290
SUMWT=C.	00001300
NH(1)=NHC	00001310
420 NIK=MOD(VBH+NHC-1,NTOT)+1	00001320
VIK=VBH+DELVC*FLOAT(NHC)	00001330
WT=CONST1/H*EXP(-SGL(VI-VIK)**2*CONST2/H**2)	00001340
CONVT=CONVT+WT*T(NIK)	00001350
SUMWT=SUMWT+WT	00001360
NHC=NHC-NST	00001370
IF(NHC.LT.0) GOTO 510	00001380
500 GO TO 420	00001390

510	SUMWT2=SUMWT	00001400
	TK0=CONVT	00001410
	IF(NTST.EQ.1) WRITE(13,9013) TK0	00001420
9013	FORMAT(' ', 5(E14.7,1X))	00001430
	NWL=2	00001440
520	IF(NWL-1+NO.GT.NM) GOTO 1310	00001450
	NST=NSTW(NWL)	00001460
	K=VH(NWL)+NST	00001470
530	VK=VBH+DELVC*FLOAT(K)	00001480
	IT=(K-GE.NTOT) GOTO 810	00001490
	ABSK=C.	00001500
	DO 600 L1=1,NLINES	00001510
	L=IACTV(MOD(ITAIL+L1-2,LINTCP)+1)	00001520
	MOLNML=MOLNM(L)	00001530
	SOL=SC(L)	00001540
	VOL=(VK-VG(L))*ALN2	00001550
	ALLL=ALL(L)	00001560
	AMASL=AMAS(L)	00001570
	EPPL=EPP(L)	00001580
	NPARTL=NPART(MOLNML)	00001590
	DO 700 IAT=1,NLEVL5	00001600
	TEMP=TMP(IAT)	00001610
	RT=TO/TEMP	00001620
	ALD=AMASL*SQRT(TEMP)	00001630
	BOLT=SQRT(RT**NPARTL)*EXP(EPPL*(RT-1.))	00001640
	AK0=U(IAT)*SOL*BOLT/ALD*RMIXR(MOLNML,IAT)	00001650
	Y=ALLL*PRES(IAT)/TEMP	00001660
	X=VOL/ALD	00001670
	ZH=DCMPLX(Y,-X)	00001680
	F=(((((A0*ZH+A5)*ZH+A4)*ZH+A3)*ZH+A2)*ZH+A1)*ZH+A0)	00001690
	Z/((((((ZH+B6)*ZH+B5)*ZH+B4)*ZH+B3)*ZH+B2)*ZH+B1)*ZH+B0)	00001700
	ZVOIGT=F	00001710
	DZABS=AK0*ZVOIGT	00001720
	ABSK=ABSK+DZABS	00001730
700	CONTINUE	00001740
	IF(ABSK.GT.TTOP) GOTO 610	00001750
600	CONTINUE	00001760
610	NK=MOD(NBH+K-1,NTGT)+1	00001770
	T(NK)=DEXP(-ABSK)	00001780
C	IF(NTST.EQ.2) WRITE(14,9014) T(NK),VK	00001790
	K=K+NST	00001800
800	GO TO 530	00001810
810	NHC=K-NST	00001820
	CONVT=C.	00001830
	SUMWT=C.	00001840
	NH(NWL)=NHC	00001850
820	NIK=MOD(NBH+NHC-1,NTOT)+1	00001860
	VIK=VBH+DELVC*FLOAT(NHC)	00001870
	WT=CONST1/H*EXP(-SMGL(VI-VIK)**2*CONST2/H**2)	00001880
	CONVT=CONVT+WT*T(NIK)	00001890
	SUMWT=SUMWT+WT	00001900
	NHC=NHC+NST	00001910
	IF(NHC.LT.0) GOTO 910	00001920
900	GO TO 820	00001930
910	SUMWT2=SUMWT2+SUMWT	00001940
	CONVT=CONVT/LOAT(2**((NWL-2)))	00001950
	IF(NWL.LE.2) GOTO 1010	00001960
	NSTUPR=NWL-2	00001970
	DO 1000 NCR=1,NSTUPR	00001980
	FNCR=FLOAT(4**NCR)	00001990
	AMKN=(FNCR*CONVT-AMK(NCR))/(FNCR-1.)	00002000
	AMK(NCR)=CONVT	00002010

CONVT=AMKN	00002020
1000 CONTINUE	00002030
1010 AMK(NWL-1)=CONVT	00002040
AMTS=ABS(TKO-CONVT)	00002050
IF(AMTS.LE.EPA) GOTO 1110	00002060
DAVF=FLOAT(2*4**((NWL-2)-1)/FLCAT(4**((NWL-1)-1))	00002070
TKO=CONVT+DAVF*(TKO-CONVT)	00002080
IF(NTST.EQ.1) WRITE(13,9013) AMK,TKO	00002090
NWL=NWL+1	00002100
1100 GO TO 523	00002110
1110 TCI(I)=FLOAT(NSTW(1)/2)*DELVC*(CONVT+TKO)	00002120
IF(NTST.EQ.1) WRITE(13,9013) AMK	00002130
1120 IF(I.GE.NVO) RETURN	00002140
I=I+1	00002150
VI=VL+FLOAT(I-1)*(VJ-VL)/FLCAT(NVC-1)	00002160
VDBH=(VI-VBH)/DELVC-FLOAT((NTCT-1)/2)	00002170
IF(VDBH.GE.FLOAT(NTOT-1)) GOTO 12C	00002180
NDBH=INT(VDBH)	00002190
NBH=MUD(NBH+NDBH-1,NTCT)+1	00002200
VBH=VBH+DELVC*FLOAT(NDBH)	00002210
JSTOP=NH-NO+1	00002220
DO 1200 J=1,JSTOP	00002230
NH(J)=NH(J)-NDBH	00002240
1200 CONTINUE	00002250
NCH=1	00002260
NST=NSTW(1)	00002270
1490 NHH=NH(NCH)	00002280
1500 IF(NHH.GE.NST) GOTO 1510	00002290
NHH=NHH+NST	00002300
GO TO 1500	00002310
1510 NH(NCH)=NHH	00002320
1520 NCH=NCH+1	00002330
IF(NCH.GT.(NM-NO+1)) GOTO 1600	00002340
NST=NSTW(NCH)	00002350
GO TO 1490	00002360
1600 CONTINUE	00002370
GO TO 130	00002380
1310 TCI(I)=TKO*DELVC*FLOAT(NSTW(1))	00002390
CALL ERROR(11,C)	
GO TO 1120	00002400
1320 TCI(I)=1.C	00002410
CALL ERROR(12,C)	
GO TO 1120	00002420
1330 ASSIGN 136 TO ISWT	00002430
VONXT=CANXT+VU+10.*H*EXTNT	00002440
GO TO 138	00002450
1340 CALL ERROR(13,C)	
ITAIL=MGD(ITAIL+LINTOP-NLINES-1,LINTOP)+1	
NLINES=LINTOP	
9912 FORMAT(' ERROR IN LINE SORTER')	00002470
GO TO 134	
1350 CALL ERROR(14,C)	
RETURN	00002480
END	00002490
SUBROUTINE ERROR(I,J)	
DIMENSION IER(50)	
COMMON /ERR/ N,M11,IER	
IF (J.NE.0) GOTO 1000	
IF (I.EQ.11) GOTO 500	
N=N+1	
IER(N)=I	
RETURN	


```

500 M11=M11+1
   RETURN
1000 WRITE(6,*) M11,IER
   RETURN
   END

```

```

/*
//GL.SYSLIN DD DSN=TSC462.NSPEC.OBJ,DISP=SHR
//GU.FT10F001 DD DSN=TSC462.SNIDER.DATA(SAVE),DISP=SHR
//GU.FT11F001 DD DSN=TSC462.LINPAR.DATA,DISP=SHR
//GU.FT12F001 DD SYSCUT=A
//GU.FT13F001 DD SYSCUT=A
//GU.SY5IN DD *
190 45.0 95.0 45.0 15 11
3.89E-06 322.0E-06 0.0 0.0 0.0
1900.0 1900.05 2 7 1 0.005 5.5 0.05 200 10.0 0
/*
//

```

APPENDIX B

THE LINE PARAMETER SETUP PROGRAM

This program reads the AFGL line listing tape and creates a file of selected line parameters. The two-step JCL routine runs the FORTRAN program to read and select the line parameters and then calls for an all core sort using the IBM system sort routine to put the lines in increasing order of the lowest frequency value at which they have significant absorption. A sample of the line parameter output after sorting is also included. As written, the program selects N₂O lines from 2550 - 2560 cm⁻¹ for a ground-based observer looking straight up at the sun. The line parameter listing example is for a different case.

```

00010 // REGION=192K,TIME=2
00020 //XSETUP UNIT=TAPE9,ID=(AFCRL,J229,READ)
00030 //NTAPE EXEC FORTRUN,TIME=2,REGION=192K
00035 //CMP.SYSRINT DD SYSOUT=X
00040 //CMP.SYSIN DD DSN=TS0462.BOB.FORT,DISP=SHR
00045 //GO.SYSLDUT DD SYSOUT=X
00050 //GO.FT09F001 DD LABEL=(1,BLP,,IN),
00060 // UNIT=TAPE9,VOL=SER=AFCRL,DISP=(OLD,KEEP),DCB=(LRECL=3200,RECFM
=FB,
00070 // BLKSIZE=3200)
00080 //GO.FT10F001 DD LABEL=(2,BLP,,IN),
00090 // UNIT=TAPE9,VOL=SER=AFCRL,DISP=(OLD,KEEP),DCB=(LRECL=3200,RECFM
=FB,
00100 // BLKSIZE=3200)
00110 //GO.FT11F001 DD LABEL=(3,BLP,,IN),
00120 // UNIT=TAPE9,VOL=SER=AFCRL,DISP=(OLD,KEEP),DCB=(LRECL=3200,RECFM
=FB,
00130 // BLKSIZE=3200)
00140 //GO.FT12F001 DD LABEL=(4,BLP,,IN),
00150 // UNIT=TAPE9,VOL=SER=AFCRL,DISP=(OLD,KEEP),DCB=(LRECL=3200,RECFM
=FB,
00160 // BLKSIZE=3200)
00170 //GO.FT13F001 DD LABEL=(5,BLP,,IN),
00180 // UNIT=TAPE9,VOL=SER=AFCRL,DISP=(OLD,KEEP),DCB=(LRECL=3200,RECFM
=FB,
00190 // BLKSIZE=3200)
00200 //GO.FT14F001 DD DSN=&&LINE,DISP=(MOD,PASS),UNIT=SYSDA,
00210 // SPACE=(TRK,(1,1)),DCB=(RECFM=FB,LRECL=42,BLKSIZE=2100)
00220 //S EXEC SORT
00230 //S.SORTIN DD DSN=&&LINE,DISP=(OLD,DELETE)
00240 //S.SORTOUT DD DSN=TS0462.L2.DATA,DISP=SHR
00250 //S.SYSIN DD *
00260 SORT FIELDS=(1,9,CH,A),SIZE=E200
END OF DATA

```

```

00010 DIMENSION G(40), SS(40), AP(40), A(9, 40), ISOT(40), MOL(40),
00020 # ID(40), EE(40), UM(6), EPSLON(2)
00030 INTEGER TOPE
00040 REAL*8 G
00050 DATA UINIT, UFINAL, BOUND, H, DEPTH
00060 # /2550.0, 2560.0, 2.0, .30, 0.010/
00070 KOUNT = 0
00080 UBOT = UINIT - (BOUND + H)
00090 UTOP = UFINAL + (BOUND + H)
00100 UM(4)=5.80E18
00110 P=1.0
00120 EPSLON(1)=DEPTH/UM(1)*3.1415927*P
00130 EPSLON(2)=DEPTH/UM(2)*3.1415927*P
00140 MF = 9
00150 IF (UBOT .GT. 500.0) MF = 10
00160 IF (UBOT .GT. 1000.0) MF = 11
00170 IF (UBOT .GT. 2000.0) MF = 12
00180 IF (UBOT .GT. 5000.0) MF = 13
00190
00200 3 REWIND MF
00210 1 CONTINUE
00220 READ (MF, 2, END=6, ERR=4) (G(I), SS(I), AP(I), EE(I), (A(J,
I),
00230 @ J = 1, 9), ID(I), ISOT(I), MOL(I), I = 1, 40)
00240 2 FORMAT (40(F10.3, E10.3, F5.3, F10.3, 8A4, A3, I3, I4, I3))
00250 IF (G(40) .LT. UBOT) GO TO 1
00260 IF (G(1) .GT. UTOP) GO TO 9
00270 DO 2002 I = 1, 40
00280 IF (MOL(I).NE.4) GO TO 2002
00290 IF (SS(I)/AP(I).LT.EPSLON(MOL(I))) GO TO 2002
00300 KOUNT = KOUNT + 1
00310 CENTU=SQRT(SS(I)*UM(MOL(I))*AP(I)*P/3.1415927/0.0001
00320 #-(AP(I)*P)**2)
00321 IG=G(I)*1.0D3
00331 IC=CENTU*1000.0
00331

```

```

00341      G(I)=DFLOAT(IG-IC)/1.0D3
00351      CENTW=FLOAT(IC)/1000.0
00352      WRITE(14,100) G(I),SS(I),AP(I),EE(I),MOL(I),CENTW
00353      100  FORMAT(F9.3,E10.3,F6.3,F9.3,I2,F6.3)
00354      IF (KOUNT .GE. 200) GO TO 9
00355      2002 CONTINUE
00360          GO TO 1
00370      6  MF = MF + 1
00380          GO TO 3
00390      4  WRITE (6, 605) MF
00400      605 FORMAT('0 ERROR ON UNIT #', I3)
00410      9  CONTINUE
00420      STOP
00430      END

```

1893.333	0.815E-20	0.077	504.000	116.277
1893.333	0.121E-21	0.041	1216.200	1 1.446
1893.345	0.403E-22	0.041	1216.200	1 0.834
1893.338	0.910E-23	0.044	1411.650	1 1.301
1893.417	0.494E-23	0.063	994.190	2 1.301
1893.530	0.557E-25	0.075	48.596	2 0.150
1893.545	0.113E-22	0.007	2661.050	1 0.185
1893.624	0.392E-23	0.007	2661.050	1 0.106
1893.775	0.398E-25	0.074	1429.125	2 0.124
1893.854	0.122E-23	0.069	1054.764	2 0.677
1893.859	0.303E-22	0.044	1411.680	1 0.751
1893.932	0.680E-23	0.050	2144.120	1 0.378
1893.999	0.126E-23	0.069	1031.127	2 0.688
1894.205	0.715E-25	0.070	2764.710	1 0.045
1894.271	0.484E-25	0.075	40.497	2 0.140
1894.291	0.466E-22	0.047	1631.410	1 0.959
1894.456	0.919E-25	0.074	2398.390	1 0.053
1894.468	0.301E-24	0.053	2337.700	1 0.082
1894.492	0.315E-22	0.059	1843.020	1 0.887
1894.535	0.349E-25	0.074	1417.376	2 0.118
1894.586	0.249E-23	0.099	221.234	1 0.322
1894.678	0.648E-23	0.064	917.056	2 1.502
1894.823	0.991E-25	0.053	2337.530	1 0.047
1894.838	0.155E-22	0.046	1631.270	1 0.551
1894.855	0.207E-24	0.073	786.903	2 0.286
1894.868	0.640E-23	0.049	1875.530	1 0.362
1894.894	0.864E-26	0.010	2952.700	1 0.005
1894.970	0.107E-26	0.075	2046.403	2 0.020
1894.991	0.115E-26	0.075	2055.035	2 0.021
1895.012	0.412E-25	0.075	33.134	2 0.129
1895.015	0.121E-26	0.074	2064.452	2 0.021
1895.040	0.126E-26	0.074	2074.654	2 0.022
1895.069	0.129E-26	0.074	2085.640	2 0.022

Blank
Page
80

REFERENCES

1. Chang, Y. S, and Shaw, J. H., Applied Spectroscopy 31, 213 (1977).
2. Armstrong, B. H., J. Quant. Spectrosc. Radiat. Transfer 7, 61 (1967).
3. Drayson, S. R., J. Quant. Spectrosc. Radiat. Transfer 16, 611 (1976).
4. Handbook of Optics, Walter G. Driscoll, Ed., McGraw-Hill, New York (1978).
5. Bouguer, P., "Essai d'optique sur la gradation de la lumière," Claude Tombert, Paris (1729).
6. Beer, A., Ann. Phys. Chem. 86(2), 78 (1852).
7. Treve, Y., "New Values of the Optical Airmass and the Refraction and Comparison with Previous Tables," Technical Report ESD-TDR-64-103, Mitre Corporation (1964).
8. Treve, Y., "A New Method for the Calculation of the Atmospheric Refraction and the Optical Airmass," (unpublished).
9. Snider, D. E., "Refractive Effects in Remote Sensing of the Atmosphere with Infrared Transmission Spectroscopy," J. Atmos. Sci. 32, 2178 (1975).
10. Snider, D., and Goldman, A., "Refractive Effects in Remote Sensing of the Atmosphere with Infrared Transmission Spectroscopy," USA Ballistic Research Lab. Report 1790 (1975).
11. Goody, R., Atmospheric Radiation, Oxford, London (1964).
12. Merzbacker, E., Quantum Mechanics, McGraw-Hill, New York (1968)..
13. Herzberg, G., Molecular Spectra and Molecular Structure II. Infrared and Raman Spectra of Polyatomic Molecules, Van Nostrand, New York, 505 (1945).
14. McClatchey, R. A.; Benedict, W. S.; Clough, S. A.; Burch, D. E.; Calfee, R. F.; Fox, K.; Rothman, L. S.; and Garing, J.S., "AFCRL Atmospheric Absorption Line Parameters Compilation" Air Force Cambridge Research Laboratories, Environmental Research Papers, No. 434, AFCRL-TR-73-0096 (1973).
15. von Planta, P., J. Opt. Soc. Amer. 47, 629-631 (1957).
16. Marten, A., Baluteau, J., and Bussoletti, E., Infrared Physics 17, 197-224 (1977).

17. Mankin, W., Applied Optics (1979) (to be published).
18. Pierluissi, J. H., and Vanderwood, P. C., J. Quant. Radiat. Transfer 18, 555-558 (1977).
19. Davis, P. J., and Rabinowitz, P., Numerical Integration, Blaisdell Pub., Waltham, Massachusetts (1967).
20. Cole, A. E., and Kantor, A. J., Air Force Reference Atmospheres, AFGL Report No. AFGL-TR-78-0051 (1978).
21. U.S. Standard Atmosphere, 1976, NOAA-S/T-76-1562.
22. Schmidt, W., Remote Sensing of the Atmosphere: Inversion Methods and Applications, Alain L. Fymot and Vladimir E. Zuev, Ed., Elsevier, Amsterdam, 149 (1978).
23. Hui, A. K.; Armstrong, B. H.; and Wray, A. A., J. Quant. Spectrosc. Radiat. Transfer 19, 509-516 (1978).
24. Young, C., Tables for Calculating the Voigt Profile, University of Michigan, Department of Engineering Technical Report No. 058673-7-T (1965).
25. Kyle, T. G., and Goldman, A., Atlas of Computed Infrared Atmospheric Absorption Spectra, NCAR Technical Note NCAR-TN/STR-112 (1975).
26. Lees, R. M., J. Mol. Spec. 33, 124-136 (1970).
27. Fisher, R. A., Statistical Methods and Scientific Inference, Oliver and Boyd, London (1956).
28. Bevington, P. R., Data Reduction and Error Analysis for the Physical Sciences, McGraw-Hill, New York (1969).
29. Smirnov, V. I., Linear Algebra and Group Theory, Dover, New York, sec 39, (1961).
30. Mill, J. D., and Drayson, S. R., Remote Sensing of the Atmosphere: Inversion Methods and Applications, Alain L. Fymot and Vladimir E. Zuev, Ed., Elsevier, Amsterdam, 123-148 (1978).